HHS Public Access

Author manuscript

J Leukoc Biol. Author manuscript; available in PMC 2022 January 01.

Published in final edited form as:

J Leukoc Biol. 2022 January ; 111(1): 33–49. doi:10.1002/JLB.3MIA0321-150RR.

Plasma extracellular vesicles released after severe burn injury modulate macrophage phenotype and function

Micah L. Willis[1], **Cressida Mahung**[2], **Shannon M. Wallet**[3,4], **Alexandra Barnett**[5], **Bruce A. Cairns**[1,2,4], **Leon G. Coleman Jr.**[5], **Robert Maile**[1,2,4]

[1]Curriculum in Toxicology and Environmental Medicine, University of North Carolina at Chapel Hill, Chapel Hill, North Carolina, USA

[2]North Carolina Jaycee Burn Center, Department of Surgery, University of North Carolina at Chapel Hill, Chapel Hill, North Carolina, USA

[3]Adams School of Dentistry, Division of Oral and Craniofacial Health Sciences, University of North Carolina at Chapel Hill, Chapel Hill, North Carolina, USA

[4]Department of Microbiology and Immunology, University of North Carolina at Chapel Hill, Chapel Hill, North Carolina, USA

[5]Department of Pharmacology, School of Medicine, University of North Carolina at Chapel Hill, Chapel Hill, North Carolina, USA

Abstract

Extracellular vesicles (EVs) have emerged as key regulators of immune function across multiple diseases. Severe burn injury is a devastating trauma with significant immune dysfunction that results in an ~12% mortality rate due to sepsis-induced organ failure, pneumonia, and other infections. Severe burn causes a biphasic immune response: an early (0–72 h) hyper-inflammatory state, with release of damage-associated molecular pattern molecules, such as high-mobility group protein 1 (HMGB1), and proinflammatory cytokines (e.g., IL-1β), followed by an immunosuppressive state (1−2+ wk post injury), associated with increased susceptibility to life-threatening infections. We have reported that early after severe burn injury HMGB1 and IL-1β are enriched in plasma EVs. Here we tested the impact of EVs isolated after burn injury on phenotypic and functional consequences in vivo and in vitro using adoptive transfers of EV. EVs isolated early from mice that underwent a 20% total body surface area burn injury (burn EVs) caused similar hallmark cytokine responses in naïve mice to those seen in burned mice. Burn EVs transferred to RAW264.7 macrophages caused similar functional (i.e., cytokine secretion) and immune gene expression changes seen with their associated phase of post-burn immune dysfunction. Burn EVs

Correspondence Leon Coleman, Assistant Professor, 1007C Thurston Bowles Bldg.,CB7178,Chapel Hill, NC27599, USA. leon_coleman@med.unc.edu; Robert Maile, Associate Professor, 8031 BurnettWomack,Chapel Hill, NC27588, USA. robmaile@med.unc.edu.

AUTHORSHIP

The authors were involvedin the following manner: conceptualization, R.M./L.G.C./S.M.W.; investigation, M.W./R.M./C.M./A.B.; data curation—formal analysis, R.M./M.W./L.G.C.; project administration/oversight, R.M./L.G.C./S.M.W./B.A.C.; writing—original draft, R.M./S.M.W./L.G.C./M.W.; and writing—review, editing, and revision, R.M./S.M.W./L.G.C./C.M./M.W.

Leon Coleman and Robert Maile contributed equally to this work.

DISCLOSURES

The authors declare no conflicts of interest.

isolated early (24 h) induced MCP-1, IL-12p70, and IFNγ, whereas EVs isolated later blunted RAW proinflammatory responses to bacterial endotoxin (LPS). We also describe significantly increased HMGB1 cargo in burn EVs purified days 1 to 7 after injury. Thus, burn EVs cause immune outcomes in naïve mice and macrophages similar to findings after severe burn injury, suggesting EVs promote post-burn immune dysfunction.

Graphical Abstract

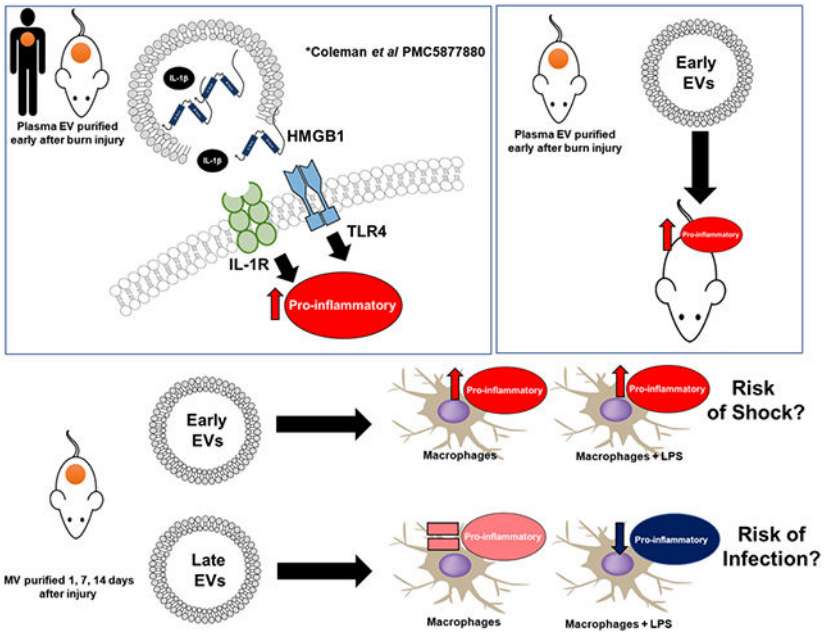

Keywords

burn injury; extracellular vesicles; macrophages; thermal injury

1 | INTRODUCTION

Severe burn injury is one of the most devastating forms of trauma, with mortality rates reaching up to 12% even in specialized burn centers.[1-3] In the United States approximately 450,000 burn injuries occur each year that require medical treatment with nearly 3500 deaths.[1-3] Mortality due to severe burn injury is primarily due to complications such as organ failure, pneumonia, and infections of other organs.[4-11] The majority of these complications occur days to weeks after repair of the skin barrier function by skin grafting.[12] This organ/tissue damage and increased vulnerability to infections is connected to the persistent immune dysfunction caused by severe burn injury.[13]

It is generally accepted that burn injury results in a biphasic systemic immune dysfunction.[14-21] The acute phase (0–72 h post injury) is referred to as burn shock or systemic inflammatory response syndrome, and can lead to barrier dysfunction and multiple organ failure in the early time points after injury.[22] In most patients who survive this early period, it is clinically obvious they enter a late/chronic phase of immune dysfunction

(beginning 1–2 wk after burn) associated with an increased susceptibility to infection referred to as the compensatory anti-inflammatory response syndrome.[23,24] However, due to the heterogeneity of these responses we and other groups often refer to these phases as a mixed agonist response syndrome (MARS[23,25-30]).

Several groups including ours have shown that burn injury generates tissue damage and subsequently numerous damage-associated molecular patterns (DAMPs), such as dsDNA, hyaluronic acid (HA), high-mobility group protein 1 (HMGB1), and the microRNA Let-7 are released.[14,15,17,20,21,31-33] DAMPs engage pattern recognition receptors (PRR), including TLR, resulting in the activation of genes responsible for immune modulation, immune cell recruitment, local tissue damage, and susceptibility to infection observed in the MARS following burn injury.[14,15,17,34-40] We have previously shown the pattern of macrophage TLR expression is highly dynamic after burn injury, with expression significantly increased within the first three days of burn injury, returning to normal levels at day 7 and then gene and protein levels of multiple TLRs undetectable on macrophages by day 14 after burn injury.[15] Unfortunately, attempts to modulate these phases of immune dysfunction with cytokine/anti-cytokine therapy have largely been unsuccessful,[41-44] suggesting additional multimodal immunologic interactions also play a role in driving clinical disease.

Extracellular vesicles (EVs) have emerged as novel mediators of immune dysfunction across several immune pathologies, including burn injury.[45-49] EVs are continuously released from nearly all cell types into biologic fluids including plasma whereby their frequency and composition changes under pathologic conditions.[50] EVs are classified primarily based on their size and biogenesis into three main categories: apoptotic bodies (>1 μm), microvesicles (~0.1–1 μm), and exosomes (~50–100 nm). There is some overlap in size, cargo, and surface markers between exosomes and EVs, though exosomes originate from the endosomal system whereas EVs primarily arise from budding from cell surface membranes.[46-49,51] We have previously reported EVs, but not EV-depleted plasma, is progressively enriched in the DAMP HMGB1 during the first 72 h after severe burn injury in both mice and humans.[17] This was associated with a parallel increase in EV-associated IL-1β and the formation of immunopotent HMGB1-IL-1β complexes.[17,52,53]

In this study, we hypothesized that EV release after burn injury is biphasic whereby those released early following burn injury promote proinflammatory and tissue damaging responses, and those released at later stages post-burn contribute to the impaired responses to infection. To test this hypothesis, we evaluated the phenotypic and functional consequences of burn-induced EVs in vivo and in vitro. Specifically, we performed adoptive transfers of EVs isolated from mice early after burn to naïve uninjured mice and evaluated the effect on plasma cytokine responses. As macrophages are players in both early and late post-burn immune dysfunction the effect of burn-induced EVs on macrophage activation and function were determined. Macrophages were exposed to burn-induced EVs isolated during the early or late post-burn immune phases and subsequent cytokine production, innate immune gene induction, and bacterial endotoxin (LPS) induced phagocytosis were evaluated. We also describe increased HMGB1 cargo in the days 1–7 burn EVs. Together, the data presented here demonstrate that EVs secreted early and late after burn injury

recapitulate many of the immune responses responsible for the biphasic MARS due to profound immunoregulatory effects on macrophages. This work implicates EVs as drivers of both phases of immune dysfunction after burn injury and thus identifies EVs as novel therapeutic targets in the treatment of severe burn injury.

2 | METHODS

2.1 | Mouse 20% total body surface area (TBSA) burn injury model

All protocols were performed in strict accordance with the Guide for the Care and Use of Laboratory Animals of the National Institute of Health. The study protocol was approved by the University of North Carolina Institutional Animal Care and Use Committee (#18–118) with ethically appropriate experimental design; all animals were housed in American Association for Accreditation of Laboratory Animal Care (an international private, nonprofit organization that promotes the humane treatment of animals in science through voluntary accreditation and assessment programs) accredited facilities with full time veterinarians on staff. Close observation of animals was performed at all times. All appropriate measures were followed to alleviate suffering. All burns and sham injuries were performed under general anesthesia. Mice underwent a 20% TBSA thermal injury as described previously.[14] Briefly, female, C57B/6 mice (6–8 wk old, 15–20 g) were anesthetized with tribromoethanol (avertin; 475 mg/kg) and their dorsum shaved before injection of subcutaneous morphine sulfate (3 mg/kg). After which four separate areas of skin were subjected to 10 s exposures to a copper rod heated to 100°C in a water bath, resulting in a full-thickness 20% TBSA burn. Mice were resuscitated with Ringer's lactate solution (0.1ml/g body weight). Ongoing pain control was provided ad lib through morphine sulfate-supplemented water (60 μg/20 g mouse) throughout the experimental period. Sham-treated mice received the same treatment and pain medication without heated copper rod application. Mice were monitored at least twice a day for the first 48–72 h post procedure or until they are stabilized. Once the mice were stable, they were monitored every other day. If mice developed overt symptoms of trauma and if not easily treated for their illness (hunched, dehydrated, struggling with breathing, lost >15% body weight, were inactive, or suffered lesions) they were euthanized immediately using inhaled isoflurane (drop method), followed by cervical dislocation. There were never any unexpected deaths.

2.2 | EV isolation, quantification, and sizing

EVs were isolated from plasma of mice 1, 7, and 14 d post-burn injury by sequential centrifugation as described previously.[17,54] Briefly, mice were euthanized by inhaled isoflurane, blood recovered by cardiac puncture, and placed in heparin containing tubes for plasma isolation. Plasma was centrifuged at 2000 ×*g* for 20 min to remove cells. Supernatant was then centrifuged at 10,000 ×*g* for 30 min to remove cellular debris. Remaining supernatant was then centrifuged at 21,000 ×*g* for 1 h. The EV-containing pellet was washed in PBS and centrifuged again at 21,000 ×*g*. This preparation results in EVs ranging between 100 nm and 1 μm in diameter.[54] EV pellets were resuspended in 2–3 ml of saline, filtered with a 0.22 μM syringe filter, and frozen at −80°C. Nanoparticle tracking analysis (NTA) was performed on the final EV products using the ZetaView QUATT instrument (Particle Metrix, Mebane, NC) and ZetaView (version 8.05) software. Mean concentrations (EV/ml)

and mode size (diameter in nanometers) were determined from 10 videos taken of one sample analyzed at a 1:1000 dilution with filtered PBS with a 488 nm laser, pump speed 30, camera shutter of 100. Each measurement obtained from the 10 videos was internally quality controlled by the instrument, with videos removed for failing quality control.

2.3 | ELISA measurements of plasma EV-bound HMGB1

HMGB1 levels were determined in EVs by ELISA according to the manufacturer's instruction with modification. EVs derived from plasma samples were diluted 1:25 in Tris lysis buffer containing 7.4% EDTA, 3.8% EGTA, and 1% Triton X-100 to release EV associated cargo. Samples were then treated with perchloric acid to liberate HMGB1 from its binding partners to allow for measurement of total HMGB1 as previously described and ELISA performed according to manufacturer's instructions.[55] Resultant samples had protein concentrations of EVs assessed using a BCA assay. HMGB1 measurements in EVs were normalized to total EV protein to account for sample variation. Previously in our laboratory we have observed that there is a Hook effect when measuring HMGB1 in plasma samples, which results in erroneously low plasma HMGB1 measurements when a low dilution factor is used. Therefore, a dilution factor of 30, optimized from our previous work, was used for all EV HMGB1 ELISA assessments.

2.4 | EV adoptive transfer

Utilizing plasma EVs pooled from six mice isolated at 48 h after injury or sham procedures, 1×10^{10} EVs in sterile PBS were adoptively transferred into naïve unburned mice via tail vein injection. We used historic data from cellular adoptive transfers to determine the number of EVs to be transferred. In our burn models, traditional cellular adoptive transfer uses 5–10% of the total WBC volume to evaluate clinical outcomes (i.e., 5×10^5 to 1×10^6 cells adoptively transferred into immunocompetent mice with a 1×10^7 total WBCs volume). Thus, here we adoptively transferred 1×10^{10} EVs, which is 5–10% of the average number of plasma EV in our mice ($1–2 \times 10^{11}$; Fig. 1A). Mice were sacrificed 24 h after transfer and plasma harvested for cytokine analysis.

2.5 | RAW cell culture and EV stimulation

RAW264.7 (ATCC, Manassas, VA, USA) human macrophages cells were allowed to grow in culture according to manufacturer's instructions using DMEM media containing 10% FBS and 1% penicillin/streptomycin at 37°C and 5% CO2. A total of 1×10^6 cells were plated in 24-well cell culture plates and allowed to adhere overnight after which cells were exposed to 3×10^7, 3×10^6, or 3×10^5 EVs in the absence or presence of LPS from *Escherichia coli* O111:B4 for 24 h. Supernatants and cellular mRNA were harvested for analyses.

2.6 | Bone marrow-derived macrophage (BMDM) culture and EV stimulation

Total bone marrow cells, which were obtained from tibia and femurs from female C57BL/6 mice, were suspended into RPMI1640 media supplemented with 10% FBS, 1% penicillin/streptomycin, and 100 ng/ml rhM-CSF at a density of 3×10^5 cells/ml in 24-well plates and cultured at 37°C and 5% CO2 for 7 d. Resultant BMDMs were exposed to 3×10^7 EVs from burn or sham-injured mice for 24 h. Supernatants were harvested for analyses.

2.7 | Cytokine and chemokine detection and quantification

Bio-Plex Multi-Plex immunoassays (Hercules, CA, USA) were used to probe cell murine plasma or culture supernatants for IL-1β, IL-2, IL-6, IL-8, IL-10, IL-12(p70), IFN-g, MCP-1, and TNFα, according to the manufacturer protocols. Data were acquired on a Bio-plex 200 system running Bio-Plex Manager and Bio-Plex Data Pro Software and analyzed using a five parameter logistic spline-curve fitting method. All data are presented as picograms per milliliter.

2.8 | Immune gene detection and quantification

Isolation of mRNA was performed as previously.[17] Briefly, RAW macrophages were lysed with TRIZOL buffer (Sigma, Burlington, MA, USA) and total RNA was isolated by chloroform extraction and quantified using a nanodrop 2000 spectrophotometer. NanoString technology and the nCounter Mouse Immunology Panel (Nanostring, Seattle, WA, USA) was used to simultaneous evaluate 561 mRNAs in each sample.[56] Each sample was run in triplicate. Briefly, a total of 100 ng mRNA was hybridized to report-capture probe pairs (CodeSets) at 65°C for 18 h. After this solution-phase hybridization, the nCounter Prep Station was used to remove excess probe, align the probe/target complexes, and immobilize these complexes in the nCounter cartridge. The nCounter cartridge was then placed in a digital analyzer for image acquisition and data processing. Hundreds of thousands of color codes designating mRNA targets of interest were directly imaged on the surface of the cartridge. The expression level of each gene was measured by counting the number of times the color-coded barcode for that gene was detected, and the barcode counts tabulated. nSolver v4.0, an integrated analysis platform was used to generate appropriate data normalization as well as fold changes, resulting ratios and differential expression. nCounter v4.0 Advanced Analysis and Ingenuity Pathway Analysis along with robust R statistics were used to identify pathway-specific responses.[56]

2.9 | Phagocytosis quantification

A total of 2.5×10^5 RAW cells were plated in a 96-well flat bottom plate and were allowed to adhere for an hour, after which cells were then exposed to killed *E. coli* (K-12 strain), which have been labeled with the fluorescent dye fluorescein, in the presence or absence of 3×10^7 EVs and 10 μg/ml LPS from *E. coli* O111:B4. Phagocytosis was allowed to occur for 2 h, and extracellular fluorescent *E. coli* was removed by aspiration and quenched by trypan blue. Intracellular fluorescence was quantified using a BioMek plate reader 480 nm excitation and 520 nm emission, with two technical replicates and three biologic replicates.

3 | RESULTS

3.1 | Adoptive transfer of burn-induced EV, but not sham-induced EV, promotes a systemic cytokine response similar to that associated with burn injury

We have reported that early after burn injury (<72 h) in human patients or mice that there is a higher frequency of EVs loaded with immunomodulators, such as the DAMP HMGB1 and IL-1β cytokine, compared to EVs isolated from healthy humans or sham-injured mice.[17] Here we used our C57BL/6 murine model of burn injury, which models

a 20% TBSA full-thickness scald burn, to characterize the immunomodulatory effects of burn-induced EVs (burn EVs).[15] This model of burn injury results in a robust immunologic response that closely mirrors that seen in humans including the rapid elevation of systemic proinflammatory chemokines and cytokines such as MCP-1 (CCL2), IL-10, IL-6, and IFNγ.[12,20,36] As we and others have previously reported, mice undergoing this burn injury, but not sham injury, have the same elevated hallmark cytokines (MCP-1, IL-10, and IL-6) of burn injury that recapitulate those seen in humans.[7,28,34,38,42,57-61] To evaluate the immunomodulatory effect of EVs in vivo, we performed adoptive transfer studies of plasma-isolated EVs from burn or sham-injured control mice into healthy unburned C57BL/6 mice by tail vein injection (Fig. 1A). First, we isolated EVs from plasma 24 h after injury from burn mice and sham-injured control mice and characterized their frequency and size using NTA. Purified EVs from both groups were similar in their size distribution (Fig. 1B). We then transferred 10^{10} EVs from either sham or burned mice to naïve mice and mice were then sacrificed 24 h after transfer and immune dysfunction were evaluated by quantification of plasma cytokines using multiplex analysis. We observed that adoptive transfer of burn EVs induced higher circulating levels of burn-associated cytokines IFNγ, IL-6, IL-8, MCP-1, and IL-10 when compared to that induced by EVs isolated from sham-injured controls (Fig. 1C; $*P < 0.05$ with FDR correction for multiple comparisons $q = 0.03$). Other cytokines and chemokines evaluated (IL-1β, IL-2, IL-12[p70], and TNFα) were not significantly altered by adoptive transfer of burn-induced EVs when compared to those induced by EVs from sham-injured controls. Together these data suggest that burn injury induces the release of EVs, which induce immune responses in vivo in a manner similar to severe burn injury.

3.2 | Burn-induced EVs promote cytokine responses in macrophages reflective of burn-induced immune dysfunction

We, and others, have described macrophages as a key cellular component of the immune system that suffers profound immune dysfunction after burn injury.[15,17,20,36,38,40] Thus, to take the first step in investigating the mechanism of in vivo EV immunomodulation, we evaluated the macrophage specific response to burn-induced EV. We added equivalent numbers of EVs isolated from burn- or sham-injured mice (3×10^7, 3×10^6, or 3×10^5 EV/ml) to murine RAW264.7 macrophages (Fig. 2A). After 24 h, we harvested supernatant and measured cytokines and chemokines by multiplex analysis. We found that in a dose-dependent manner, which burn EVs induced significantly more secretion of MCP-1 (7.5-fold at 3×10^7, $*P < 0.05$ vs. sham EVs Fig. 2B), IL-12p70 (2-way ANOVA, main effect of treatment, $F_{1,7} = 70.45$, $****P < 0.0001$ vs. sham, Fig. 2C), IL-6 (8-fold at 3×10^7, $*P < 0.05$ vs. sham, Fig. 2D), and IFNγ (5.8-fold at 3×10^7, $*P < 0.05$ vs. sham, Fig. 2E). Other cytokines and chemokines evaluated (IL-1β, IL-2, IL-8, IL-10, and TNFα) were not significantly altered by EV exposure regardless of EV source. These data indicate that burn EVs can alter macrophage immune responses, specifically promoting similar cytokine profiles observed after adoptive transfer of burn EVs into untouched mice (Fig. 1C) as well as those that are observed experimentally and clinically early after burn injury.[12,20,36] RAW macrophage media contain ~1.7×10^{10} EVs/ml; thus, the EV stimulation used here was less than 1% of the number of EVs within the media, indicating a high level of potency of burn EVs.

3.3 | EVs from burn injury induce a unique set of immune genes in macrophages

To examine the expression of genes and immune regulatory pathways that are triggered by EVs, we employed Nanostring technology. This is an amplification-free technology that measures gene expression by counting mRNA molecules directly.[56] We utilized the commercially available Mouse Immunology Panel v3.0, which allows for 561 mRNA targets to be quantified simultaneously. We isolated mRNA from RAW264.7 cells exposed for 24 h to 3×10^5 EVs isolated from burn- or sham-injured mice. Volcano plots in Figure 3 demonstrate the change in gene expression along with its associated significance, following RAW cells exposure to either EVs from burn-injured (Fig. 3A) or sham-injured (Fig. 3B) mice relative to cells not exposed to EVs. Significantly altered genes ($P < 0.01$) are presented in Supporting Information Table S1 (data also uploaded to NCBI Gene Expression Omnibus GEO).

Evaluation of the normalized copy number of the key innate immune genes MCP-1, IL-6, MyD88, and NFkBl indicates that burn EVs, but not sham EVs, promote their up-regulation by ~17-fold (MCP-1, Fig. 4A, $^{***}P < 0.001$), ~3.3-fold (IL-6, Fig. 4B, $^{*}P < 0.05$), ~24-fold (MyD88, Fig. 4C, $^{***}P < 0.001$), and ~150-fold (NFkB1, Fig. 4D, $^{***}P < 0.001$). In addition, this analysis indicates that sham-injury induced EVs induce the down-regulation of IL-6 gene expression, whereby burn-induced EVs have no effect on its expression compared to cells not exposed to EVs (Fig. 4, 5). These data demonstrate that burn- and sham-injury induced EVs uniquely immunomodulate macrophages and that burn-induced EVs promote mRNA profiles associated with immune dysfunction known to occur following burn injury.

3.4 | EVs isolated at distinct phases of burn injury have differential cargo and immunomodulatory effects on macrophages

Burn injury has a clear and clinically described temporal effect on the immune system, with an early proinflammatory “shock” phase and a later compensatory phase associated with significant susceptibility to infection.[25] As discussed, this is not as clearly defined immunologically, and each phase comprises a mixed response of multiple immune mediators. We hypothesize that EVs are a hitherto undescribed contributor to these distinct phases. In previous studies, we have described unique time points as being associated with the “shock” phase (day 1), a homeostatic/inflection phase (day 7), and a compensatory phase (day 14) after a 20% TBSA burn in mice.[15] Therefore, we isolated EVs from the plasma 1, 7, and 14 d post-burn or sham injury and compared their frequency, size, and immunomodulatory effects on macrophages. Here we utilized both RAW264.7 cells and primary C57BL/6 BMDMs.

Using NTA we characterized the size and frequency of EVs from each time point. In terms of concentration in plasma (Fig. 5A), there were significantly fewer EV in the plasma of burn mice 1 d post injury vs. EVs in the plasma of sham mice. Conversely, there were significantly more EVs in the plasma of burn mice 7 d post injury vs. the plasma of sham mice. In addition, we determined if there were differences in the expression of the key EV cargo member, HMGB1, that we previously demonstrated to be localized within burn-induced EV.[17] Specifically, we found that HMGB1 was located within EV from sham- and burn-injury mice whereby EVs from burn mice contained significantly higher levels of

HMGB1 1 and 7 d post-injury when compared to sham mice (Fig. 5B). Conversely, by 14 d post-burn injury, EV-HMGB1 levels in burn mice were similar to those found in EV from sham mice. After purification, and similar to findings at 24 h (Fig. 1B), there were no clear differences in size distributions of plasma EVs isolated from sham and burn mice at 1 wk (Fig. 5C) and 2 wk (Fig. 5D) post-injury.

To determine the immunomodulatory effect of burn-induced EVs from each of these key stages of immune dysfunction, and of sham EVs, we exposed equivalent numbers of RAW264.7 or BMDM cells to equivalent numbers (3×10^7) of each EV population as in Figure 2A, and measured cytokine and chemokine levels in the media by multiplex analysis. We found that, in general, when comparing sham EV and burn EV, there was a differential response between the two in both cell types, and when comparing between EV isolated from different days after burn, there were also differential cytokine responses within and between each macrophage type. We found that burn EVs from days 1 and 7 post-burn injury induced higher expression of MCP-1 (Fig. 5E), IL-6 (Fig. 5F), IFNγ (Fig. 5G), and IL-12p70 (Fig. 5H) in RAW cells compared to EVs isolated from sham injury at the same time points. Similarly, in BMDM MCP-1 was increased more strongly by day 1 burn EVs but less so by days 7 and 14 burn EV; IL-12p70 also had a similar pattern. In contrast, we found that burn EVs from day 14 post-burn injury induced higher expression of MCP-1 (Fig. 5E) and IL-6 (Fig. 5F), but not IFNγ, (Fig. 5G) and IL-12p70 (Fig. 5H) when BMDMs were used as the target cell. Interestingly, significant secretion of IL-6 occurs in response to days 1, 7, and 14 burn EV by BMDMs vs. sham EV, but not by RAW cells, which only secretes IL-6 is response to days 1 and 7 burn EV. Finally, we found that burn-induced EV did not induce IFNγ in BMDMs regardless of time point post-burn injury (Fig. 5G). These data demonstrate that burn-injury induced EVs from different time points after burn injury uniquely immunomodulate both transformed and primary macrophage types, and are generally representative of profiles associated with the immune dysfunction observed at the respective phases of burn injury from which they were isolated.

3.5 | Macrophages exposed to EVs isolated at distinct phases of burn injury have differential immune gene expression reflective of the stage of immune dysfunction from which the EVs were isolated

To examine the differential induction of genes and immune regulatory pathways that are triggered by EVs from each stage of immune dysfunction following burn, we again employed Nanostring technology and the Mouse Immunology Panel v3.0. RAW264.7 macrophages were exposed for 24 h to equivalent numbers of EVs (3×10^5) isolated 1, 7, and 14 d post-burn injury. Volcano plots in Figure 6 demonstrate the change in gene expression along with its associated significance, following exposure to EVs isolated 1 d (Fig. 6A), 7 d (Fig. 6B), and 14 d (Fig. 6C) post-burn injury relative to RAW264.7 cells not exposed to EV. Significantly altered genes ($P < 0.01$) are presented in Supporting Information Table S2. Using principal components analysis (PCA) by nSolver Analysis of these gene expression data, we derived pathway scores (PS), based on the individual gene expression levels for all the measured genes within a specific pathway[62] to identify pathways active in the target cells. Generally, positive PS indicate pathways that are highly affected based on gene expression patterns observed whereas negative PS indicate

pathways which are not as affected based on gene expression patterns observed.[62] Figure 7A demonstrates the PS driven by EVs derived from each time point after burn injury was evaluated. Pathways shown are predicted with $P < 0.05$ confidence based on causal gene expression. PS driven by EVs isolated 1 d (green circles) and 14 d (red circles) post-burn injury are generally positive for many key immunologic pathways (e.g., TLR signaling, phagocytosis, chemokine signaling, etc.), indicating that they are significantly affected. Conversely, PS driven by EVs isolated 7 d post-burn injury (blue circles) are generally negative for these immunologic pathways, similar to that of untreated macrophages (open circles) indicating that these pathways were less impacted by these conditions (Fig. 7A). These data corroborate that burn-injury induced EVs from different time points after burn injury uniquely immunomodulate macrophages inducing mRNA profiles and differentially affect immunologic pathways associated with the immune dysfunction observed at the phase of burn injury at which they were isolated.

3.6 | Macrophages exposed to EVs isolated later after burn injury have reduced phagocytic ability

Aberrant macrophage cytokine and chemokine function can lead to tissue damage associated with early burn-induced immune dysfunction. Conversely, aberrant phagocytosis by macrophages, can lead to susceptibility to infection, the hallmark of immune dysfunction observed in later stages of burn injury. Thus, we evaluated the effect of EVs isolated for each time point post-burn injury on the phagocytic function of RAW264.7 macrophages in a model of bacterial infection. Cell were incubated with 10 μg/ml LPS and fluorescein-labeled killed *E. coli* (K-12 strain) cells, in the presence or absence of 3×10^7 EVs isolated 1, 7, or 14 d after burn injury or EVs isolated from sham-injured mice. Phagocytosis was allowed to proceed for 2 h and the amount of internalized *E.coli* quantified. EVs isolated from sham-injured mice had no effect on the LPS-induced phagocytic function of macrophages (Fig. 7B). Similarly, EVs isolated 1 and 7 d post-burn injury did not statistically affect the amount of phagocytosis (Fig. 7B). However, EVs isolated 14 d post-burn injury caused a significant impairment macrophages phagocytosis (Fig. 7B). This implicates late burn EVs in the known suppression of macrophage mediated phagocytosis following burn injury, which contributes to increased susceptibility to infection.

3.7 | Burn EVs isolated 2 wk after injury suppress macrophage proinflammatory responses to LPS

Increased risk of infection is a hallmark of post-burn pathology. Our data indicate an effect of burn-induced EVs on LPS-induced phagocytosis; thus, to examine the totality of EV's effect on LPS-induced genes and immune regulatory pathways we again employed Nanostring technology and the Mouse Immunology Panel v3.0. We probed mRNA from RAW264.7 macrophages stimulated for 24 h with 1 μg/ml LPS stimulation in the presence of 3×10^5 plasma EVs isolated 1, 7, or 14 d after burn injury or from sham-injured mice. Volcano plots in Figure 8 demonstrates the change in gene expression along with its associated significance, following exposure to LPS+ EVs isolated 1 d (Fig. 8A), 7 d (Fig. 8B), and 14 d (Fig. 8C) post-burn injury. In order to show changes in immune profiles across all treatments data are presented relative to LPS-stimulated macrophages without EV exposure. Significantly altered genes ($P < 0.01$) are presented in Supporting Information

Table S3. Evaluation of the normalized copy number of the key innate immune genes induced during LPS stimulation found that EVs isolated 1 and 7 d after burn have an additive effect on MCP-1 expression relative to untreated cells as well as those exposed to EVs isolated following sham injury (Fig. 9A). However, burn EVs collected at each time point post-burn suppressed LPS induction of proinflammatory IL-6 and MyD88 compared to sham EVs, with day 14 burn EVs almost completely abolishing responses to LPS (Fig. 9B). This is consistent with burn EVs at 14 d post-injury blunting macrophage responses to infection at a time when susceptibility to infection is increased.

As previously outlined, we determined PS for cells stimulated with EVs and LPS. Pathways shown in Figure 10 (predicted with $P < 0.05$ confidence) demonstrate the LPS-induced PS for key immunologic pathways (e.g., TLR signaling, phagocytosis, chemokine signaling, etc.) and the effect of EVs derived from each time point after burn injury on these LPS-induced PS. PS driven by LPS in the absence of EVs in general are negative (Fig. 10; open circles), whereby EVs isolated 1 and 7 d post-burn injury also drive LPS-induced negative PS (Fig. 10; green circles and blue circles, respectively). Conversely, EVs isolated 14 d post-burn injury drive LPS-induced PS, which are positive (Fig. 10; red circles). These data demonstrate that burn-injury induced EVs from different time points after burn injury uniquely immunomodulate LPS responsiveness of macrophages. Although PS can indicate the “general” directionality of a given pathways, it does not reveal the directionality of individual genes within each pathway. To this end, our analysis revealed that the PS of macrophages exposed with sham-induced EVs in the absence (Fig. 7A) or presence (Fig. 10) of LPS were generally positive. Thus, to begin the process of revealing mechanisms of sham-injury induced EVs and burn-induced EVs associated with our PS analysis, we performed a focused analysis on PRR, their downstream signaling pathways, and the resulting effector molecules using Ingenuity Pathway Analysis (Fig. 11). Figure 11 visualizes the positive (red) or negative (green) fold changes induced in LPS-treated macrophages by EVs isolated from sham injury (circles), 1 d (first square), 7 d (second square), or 14 d (third square). Each group was compared to LPS-stimulated macrophages in the absence of EVs to allow visualization of the effects of all three groups. For example, genes encoding proinflammatory cytokines, relative to unstimulated cells, are up-regulated by LPS alone (Fig. 11; red gene symbol in the bottom of the figure). These genes are strongly up-regulated in the presence of sham EVs (Fig. 11; ●), unchanged by EVs from days 1 and 7 post-burn (Fig. 11; ■), but are strongly down-regulated by EVs from day 14 post-burn (Fig. 11; ■). The collective data from Figure 11 indicate that not only do sham-injury induced EVs and burn-induced EVs drive unique LPS-induced responses in macrophages, but that burn-induced EVs from days 1 and 14 after injury are highly divergent in their ability to modulate the ability of macrophages to respond to PAMPs or DAMPs. Particularly, burn EVs isolated during the immunosuppressive/increased risk of infection phase (i.e., day 14) strongly suppress proinflammatory responses to bacterial endotoxin.

4 | DISCUSSION

Several studies (including our own) have reported differences in the number, composition, and/or cellular source of circulating EVs between healthy and diseased states.[17,63,64] It

has become obvious that the biologic roles in health and disease of EV are vital and wide ranging (reviewed in Tricarico et al.[65]). EVs are membrane-enclosed structures of heterogeneous size (~0.1–1 μm diameter), carrying a mixture of bioactive cell-derived lipids, proteins, and nucleic acids on their surface (composition) and enclosed within their membrane (cargo).[47] Packaging of molecules on and in vesicles prolongs their half-life, potency, cell-specificity, and/or enhance their local concentration. In addition, incorporation of molecules on and/or in EV precludes their detection by conventional methods. EVs are a class of EVs and while it has been described that EV pools are altered in burn patients and animal models,[66,67] no comprehensive investigation into their role in immune dysfunction after burn injury has been examined.

EVs are complex signaling vehicles, in that their composition and cargo likely activate innate immune responses through multiple routes (Fig. 12A). For instance, EVs can provide localized and concentrated release/presentation of DAMPs (e.g., HMGB1) or cytokines (e.g., IL-1β) to the cell surface receptors. We previously reported that burn injury induces the sustained release of EVs with cargo that includes HMGB1 and IL-1β in mice and humans (Fig. 12A).[17] Additionally, EVs can also fuse with the cell membrane and/or be endocytosed and fuse with endosomes whereby their cargo is released into the cytoplasm or endosome, respectively, and engage intracellular innate immune receptors. EVs might also carry oxidized or inflammatory lipids, which can immunomodulate immune cells.[68] Our group's published work and findings here demonstrate that burn injury induces the sustained release of EVs.[17] We have also described that EV association increases the functional immune potency of the cytokines.[17] Here we build upon these reports and present data that demonstrate EVs isolated after burn injury, but not sham injury, can transfer immune dysfunction to untouched control mice in a manner that suggests EVs might promote post-burn immune pathology seen clinically (Fig. 12B). This is in agreement with O'Dea et al. who have demonstrated that elevated levels of leukocyte- and granulocyte-derived EVs correlate with clinical assessment scores of burn severity associated with the risk of severe sepsis.[67] Healthy EVs might also be able to normalize immune dysfunction. An additional study reported that EVs isolated from bronchoalveolar lavage of uninjured mice could protect burn-injured mice from subsequent pulmonary bacterial infection.[66] Although these collective data implicate EVs as an immunomodulatory reservoir that is integral to the pathogenesis of burn injury morbidities mechanisms of immunomodulation were not elucidated.

As previously discussed, burn injury results in complex immune dysfunction with dichotomous early and late states,[14-21] whereby these dichotomous phenotypes are likely controlled by temporal release of DAMPs (e.g., HMGB1, HA) and immunomodulatory mediators (e.g., IL6, MCP1, and IL10).[14,15,17,32,34-38,40] However, in diverse clinical settings of trauma and sepsis, targeting individual DAMPs has been unsuccessful.[41-44] Here we demonstrate that early and late stages of immune dysfunction are associated with EVs of different immunomodulatory functions, which manifests as elevated plasma levels of IL6, MCP-1, and IFNγ. In addition, we demonstrate that EV isolated after burn injury have increasing amounts of HMGB1 cargo, which peaks at day 7 post injury, which at least in part contributes to the immune dysfunction observed following adoptive transfer of burn-injury induced EVs. We and others have extensively reported that these cytokines

correlate with burn severity, poor outcomes, and are key players in the immune mechanism of susceptibility to infection after burn injury.[7,28,34,38,42,57-61] It is important to note that these so-called hallmark cytokines of burn (MCP-1, IL-10, and IL-6) are also significantly elevated in the burn EV-donor mice after burn injury compared to sham-injured mice, as we and others have previously reported. Thus, it is possible that there is contaminant free cytokine remaining in the adoptively transferred EV samples, although our purification process should remove the bulk (if not all) of these soluble mediators. In addition, as we have published,[17] and in data not shown, we do see the most significant fraction of cytokines (and other immunomodulators) associated with EV, and not free in the plasma. IL-8 was also significantly elevated and this is likely related to epithelial proinflammatory response.[69] Together these data implicate EVs at least as an adjuvant if not a drive of the immune dysfunction, which manifests early following burn injury.

We, and others, have also reported that in human and preclinical studies macrophages play a key role in both early and late immune dysfunction[15,20,32,35-37,39,40,70-74] with aberrant macrophage cytokine and chemokine function leading to tissue damage associated with early burn-induced immune dysfunction. Conversely, aberrant phagocytosis by macrophages, can lead to susceptibility of infection, the hallmark of immune dysfunction observed during later stages of burn injury.[71,72,75] Indeed, we have published that burn injury results in a steady accumulation in the periphery of macrophages, which early after burn injury up-regulate the innate immune receptors TLR2 and TLR4, followed by a decrease of TLR2 and TLR4 expression late after burn injury, which resulted in temporal differences in TLR-induced cytokine responses.[14] Here we present data that EVs from burn injury induce a unique set of immune genes in macrophages compared to EVs from sham-injured mice and that EVs isolated at distinct phases of burn injury have differential immunomodulatory effects, both of which are reminiscent of the temporal immunologic phenotypes observed in our murine models of burn injury and clinically.[12,14,15,17,20,32,34-37,39,40] Together these data implicate EV-macrophage interactions in the burn-induced immune dysfunction.

A major clinical sequelae following burn injury is the susceptibility to infections. Defective bacterial clearance has been linked to alterations in the innate immune response of phagocytes such as macrophages, including suppressed cytokine expression and phagocytosis.[71,72] Pathogens are recognized by a variety of pattern recognition receptors (PRRs) whose expression and signaling can be altered by burn injury leading to hypo- or hyper-responsiveness.[76,77] In addition, macrophages that are extremely plastic, tend to be polarized into an anti-inflammatory phenotype due to PRR signaling by DAMPs released from damaged tissue.[78,79] We have previously shown the pattern of TLR expression is highly dynamic after burn injury, with gene and protein levels of multiple TLRs undetectable on macrophages by day 14 after burn injury.[15] Our new data are highly reflective of this biphasic response after burn injury, and we now demonstrate that immune gene expression by LPS-stimulated macrophages is highly influenced by exposure to EVs, whereby the time of isolation post-burn injury affects this influence (Fig. 12B). Specifically, those EVs isolated at later time points post-injury suppress LPS-induced PRR-induced signaling and cytokine expression (Fig. 9). In addition, we also demonstrate that macrophages exposed to EVs isolated later after burn injury have reduced LPS-induced

phagocytic ability, although PS analysis would insinuate that a number of phagocytosis-related pathways were up-regulated. PS do not indicate individual directionality of changes within each pathway. In other words, whereas the magnitude of the PS can indicate directionality of the pathway (i.e., activated vs. suppressed), it more accurately indicates the magnitude of how much the pathway is affected by the gene expression (i.e., a lot of genes were involved vs. few genes were involved). For example, although we found that sham EVs have similar impact to EVs from either day 1 and day 7 burn EVs on PS (Fig. 7), and that "no EV" are very similar to day 7 burn EVs, we provide data that implicate impaired bacterial uptake after exposure to day 14 burn EVs (although it is suggestive that in Fig. 7B that day 7 burn EV are also trending towards reduced phagocytosis). This is likely a reflection of other phagocytic-regulatory pathways being up-regulated by the cargo of EV, changing over time after burn injury (with day 7 representing a transition point), which is an area of active investigation by our group. As another example of this, we present similar PS for sham EVs vs. day 14 burn EVs (Fig. 10) in the presence of LPS. Indeed, individual signaling cascades are diminished when examined in more detail on molecular (Fig. 9) and causal pathway levels (Fig. 11). Again, this is likely a reflection of EV cargo changing over time after burn injury, with day 14 representing a transition point representing a time point of immune suppression to TLR ligands. Together these data implicate EV-macrophage interactions in burn-induced immune dysfunction, which we hypothesize leads to susceptibility to subsequent infections and may lead to future therapies targeting this interaction.

Although most experiments were performed with a single immune cell line rather than primary cells, we did demonstrate that EVs elicited similar cytokine patterns in RAW246.7 and BMDM cells, with day 14 EVs revealed to exert an effect on IL-6 secretion in BMDMs, but not in RAW246.7 cells. BMDMs were less prone to IFNγ secretion with burn EV compared to RAW. In patients, sustained high levels of circulating IL-6 correlate strongly with poor outcomes after burn injury,[80-82] and it is possible that BMDMs have a lower threshold to EV stimulation than RAW246.7 for IL-6 generation (and the converse for IFNγ). With that said, these data provide the rationale to evaluate additional primary cell times of both immune and no-immune origin. As another limitation, although we have provided NTA and flow cytometric analysis in this and an earlier study,[17] we are aware that the International Society for Extracellular Vesicles 2018 Guidelines suggest using electron microscopy for further validation[83] (especially true considering that NTA has been validated several times by Electron Microscopy). Similarly, the specific identity of the cargo of the EVs utilized in these studies was not elucidated beyond HMGB1 as in our previous reports.[17] Ongoing studies in the laboratory are interrogating the lipid, protein, mRNA, and miRNA cargo of burn-induced EVs across the course of burn-induced immune dysfunction and to identify cellular sources of EV origin.

Supplementary Material

Refer to Web version on PubMed Central for supplementary material.

ACKNOWLEDGMENTS

The authors thank the following sources of funding: NIH NIGMS R01GM131124 (to B.A.C./R.M.), NIH NIGMS 5T32GM008450 (to B.A.C./R.M./C.M.), NIH NIEHS T32ES007126 (to M.W.), NIH NIAAA AA024829-03 (to L.G.C./A.B.), and the UNC North Carolina Jaycee Burn Center Trust. They also thank the staff of the UNC Delta Translational Services Recharge Center.

Abbreviations:

DAMPs	Damage-associated molecular patterns
EVs	Extracellular vesicles
HA	Hyaluronic acid
HMGB1	High-mobility group protein 1
MARS	Mixed agonist response syndrome
NTA	Nanoparticle tracking analysis
PRR	Pattern recognition receptors
TBSA	Total body surface area

REFERENCES

1. Peck MMJ, Swart D. A global plan for burn prevention and care. Bull World Health Organ. 2009;87:802–803. [PubMed: 19876549]
2. Repository ABANB. Burn incidence and treatment in the United States: 2011 Fact Sheet In: Association AB, editor. http://ameriburn.org/resources_factsheet.php2011
3. Miller SF, Bessey P, Lentz CW, Jeng JC, Schurr M, Browning S. National burn repository 2007 report: a synopsis of the 2007 call for data. J Burn Care Res. 2008;29:862–870. discussion 71. Epub 2008/11/11. PubMed PMID: 18997556. [PubMed: 18997556]
4. Brusselaers N, Logie D, Vogelaers D, Monstrey S, Blot S. Burns, inhalation injury and ventilator-associated pneumonia: value of routine surveillance cultures. Burns. 2012;38:364–370. PubMed PMID: 22040929. [PubMed: 22040929]
5. Chen MC, Chen MH, Wen BS, Lee MH, Ma H. The impact of inhalation injury in patients with small and moderate burns. Burns. 2014;40:1481–1486. PubMed PMID: 25239845. [PubMed: 25239845]
6. Cioffi WG. What's new in burns and metabolism. J Am Coll Surg. 2001;192:241–254. [PubMed: 11220727]
7. Jeschke MG, Gauglitz GG, Kulp GA, et al. Long-term persistance of the pathophysiologic response to severe burn injury. PLoS One. 2011;6:e21245. PubMed PMID: 21789167; PMCID: PMC3138751. [PubMed: 21789167]
8. Pruitt BA Jr., Wolf SE. An historical perspective on advances in burn care over the past 100 years. Clin Plast Surg. 2009;36:527–545. PubMed PMID: 19793549. [PubMed: 19793549]
9. Strassle PD, Williams FN, Napravnik S, et al. Improved survival of patients with extensive burns: trends in patient characteristics and mortality among burn patients in a tertiary care burn facility, 2004-2013. J Burn Care Res. 2017;38:187–193. PubMed PMID: 27775983; PMCID: PMC5393966. [PubMed: 27775983]
10. Thombs BDSV, Halonen J, Diallo A, Milner SM. The effects of preexisting medical comorbidities on mortality and length of hospital stay in acute burn injury: evidence from a national sample of 31,338 adult patients. Ann Surg. 2007;245:629–634. [PubMed: 17414613]

11. Veeravagu A, Yoon BC, Jiang B, et al. National trends in burn and inhalation injury in burn patients: results of analysis of the nationwide inpatient sample database. J Burn Care Res. 2015;36:258–265. PubMed PMID: 24918946. [PubMed: 24918946]
12. van Duin D, Strassle PD, DiBiase LM, et al. Timeline of health care-associated infections and pathogens after burn injuries. Am J Infect Control. 2016. PubMed PMID: 27742146.
13. Snell JA, Loh NH, Mahambrey T, Shokrollahi K. Clinical review: the critical care management of the burn patient. Crit Care. 2013;17:241. PubMed PMID: 24093225; PMCID: PMC4057496. [PubMed: 24093225]
14. Cairns B, Maile R, Barnes CM, Frelinger JA, Meyer AA. Increased Toll-like receptor 4 expression on T cells may be a mechanism for enhanced T cell response late after burn injury. J Trauma. 2006;61:293–298. Discussion 8-9. PubMed PMID: 16917441. [PubMed: 16917441]
15. Cairns BA, Barnes CM, Mlot S, Meyer AA, Maile R. Toll-like receptor 2 and 4 ligation results in complex altered cytokine profiles early and late after burn injury. J Trauma Acute Care Surg. 2008;64:1069–1078.
16. Chen XL, Sun L, Guo F, et al. High-mobility group box-1 induces proinflammatory cytokines production of Kupffer cells through TLRs-dependent signaling pathway after burn injury. PLoS One. 2012;7:e50668. PubMed PMID: 23209806; PMCID: PMC3507775. [PubMed: 23209806]
17. Coleman LG Jr., Maile R, Jones SW, Cairns BA, Crews FT. HMGB1/IL-1beta complexes in plasma microvesicles modulate immune responses to burn injury. PLoS One. 2018;13:e0195335. Epub 2018/03/31. PubMed PMID: 29601597; PMCID: PMC5877880. [PubMed: 29601597]
18. Erridge C. Endogenous ligands of TLR2 and TLR4: agonists or assistants?. J Leukoc Biol. 2010;87:989–999. PubMed PMID: 20179153. [PubMed: 20179153]
19. Hultman CS, Cairns BA,deSerres S, Frelinger JA, Meyer AA. Early, complete burn wound excision partially restores cytotoxic T lymphocyte function. Surgery. 1995;118:421–430. [PubMed: 7638760]
20. Maile R, Jones S, Pan Y, et al. Association between early airway damage-associated molecular patterns and subsequent bacterial infection in patients with inhalational and burn injury. Am J Physiol Lung Cell Mol Physiol. 2015;308:L855–L860. PubMed PMID: 25770180; PMCID: PMC4421787. [PubMed: 25770180]
21. Rani M, Nicholson SE, Zhang Q, Schwacha MG. Damage-associated molecular patterns (DAMPs) released after burn are associated with inflammation and monocyte activation. Burns. 2017;43:297–303. PubMed PMID: 28341255; PMCID: PMC5373089. [PubMed: 28341255]
22. Nielson CB, Duethman NC, Howard JM, Moncure M, Wood JG. Burns: pathophysiology of systemic complications and current management. J Burn Care Res. 2017;38:e469–e81. PubMed PMID: 27183443; PMCID: PMC5214064. [PubMed: 27183443]
23. Finnerty CC, Jeschke MG, Herndon DN,et al. Investigators of the I, the Host Response Glue G. Temporal cytokine profiles in severely burned patients: a comparison of adults and children. Mol Med. 2008;14:553–560. doi: 10.2119/2007-00132. Finnerty. PubMed PMID: 18548133; PMCID: 2424320. [PubMed: 18548133]
24. Gauglitz GG, Song J, Herndon DN, et al. Characterization of the inflammatory response during acute and post-acute phases after severe burn. Shock. 2008;30:503–507. PubMed PMID: 18391855. [PubMed: 18391855]
25. Adib-Conquy M, Cavaillon J-M. Compensatory anti-inflammatory response syndrome. J Thromb Haemost. 2009;101:36–47.
26. Hotchkiss RS, Coopersmith CM, McDunn JE, Ferguson TA. The sepsis seesaw: tilting toward immunosuppression. Nat Med. 2009;15:496–497. [PubMed: 19424209]
27. Hur JYH, Chun W, Kim JH, Shin SH, Kang HJ, Kim HS. Inflammatory cytokines and their prognostic ability in cases of major burn injury. Ann Lab Med. 2015;35:105–110. [PubMed: 25553289]
28. Mannick JA, Rodrick ML, Lederer JA. The immunologic response to injury. J Am Coll Surg. 2001;193:237–244. [PubMed: 11548792]
29. Osuchowski MF, Craciun F, Weixelbaumer KM, Duffy ER, Remick DG. Sepsis chronically in MARS: systemic cytokine responses are always mixed regardless of the outcome, magnitude,

or phase of sepsis. J Immunol. 2012;189:4648–4656. PubMed PMID: 23008446; PMCID: PMC3478412. [PubMed: 23008446]

30. Ulloa L, Tracey KJ. The 'cytokine profile': a code for sepsis. Trends Mol Med. 2005;11:56–63. [PubMed: 15694867]
31. D'Arpa P, Leung KP. Toll-like receptor signaling in burn wound healing and scarring. Adv Wound Care. 2017;6:330–343. PubMed PMID: 29062590; PMCID: PMC5649422.
32. Dunn JLM, Kartchner LB, Gast K, et al. Mammalian target of rapamycin regulates a hyperresponsive state in pulmonary neutrophils late after burn injury. J Leukoc Biol. 2018. PubMed PMID: 29393976.
33. Zhang Y, Yin B, Shu B, Liu Z, Ding H, Jia C. Differential expression of microRNA let-7b-5p regulates burn-induced hyperglycemia. Oncotarget. 2017;8:72886–72892. PubMed PMID: 29069833; PMCID: PMC5641176. [PubMed: 29069833]
34. Jones SW, Zhou H, Ortiz-Pujols SM, et al. Bronchoscopy-derived correlates of lung injury following inhalational injuries: a prospective observational study. PLoS One. 2013;8:e64250. PubMed PMID: 23691180; PMCID: PMC3656836. [PubMed: 23691180]
35. Dunn JL, Hunter RA, Gast K, Maile R, Cairns BA, Schoenfisch MH. Direct detection of blood nitric oxide reveals a burn-dependent decrease of nitric oxide in response to *Pseudomonas aeruginosa* infection. Burns. 2016. PubMed PMID: 27268107.
36. Moore CBMM, van Deventer HW, O'Connor BP, et al. Downregulation of immune signaling genes in patients with large surface burn injury. J Burn Care Res. 2007;28:879–887. [PubMed: 17925653]
37. Neely CJ, Kartchner LB, Mendoza AE, et al. Flagellin treatment prevents increased susceptibility to systemic bacterial infection after injury by inhibiting anti-inflammatory IL-10+ IL-12- neutrophil polarization. PLoS One. 2014;9:e85623. PubMed PMID: 24454904; PMCID: 3893295. [PubMed: 24454904]
38. Eitas TK, Stepp WH,Sjeklocha L, et al. Differential regulation of innate immune cytokine production through pharmacological activation of nuclear factor-erythroid-2-related factor 2 (NRF2) in burn patient immune cells and monocytes. PLoS One. 2017;12:e0184164. PubMed PMID: 28886135; PMCID: PMC5590883. [PubMed: 28886135]
39. Dunn JLM, Kartchner LB, Stepp WH, et al. Blocking CXCL1-dependent neutrophil recruitment prevents immune damage and reduces pulmonary bacterial infection after inhalation injury. Am J Physiol Lung Cell Mol Physiol. 2018;314:L822–L34. PubMed PMID: 29368547; PMCID: 6008131. [PubMed: 29368547]
40. Kartchner LB, Gode CJ, Dunn JLM, et al. One-hit wonder: late after burn injury, granulocytes can clear one bacterial infection but cannot control a subsequent infection. Burns. 2019. PubMed PMID: 30833100.
41. Wasserman D, Ioannovich JD, Hinzmann RD, Deichsel G, Steinmann GG. Interferon-gamma in the prevention of severe burn-related infections: a European phase III multicenter trial. The Severe Burns Study Group. Crit Care Med. 1998;26:434–439. PubMed PMID: 9504568. [PubMed: 9504568]
42. Efron PA, Moldawer LL. Cytokines and wound healing: the role of cytokine and anticytokine therapy in the repair response. J Burn Care Rehabil. 2004;25:149–160. PubMed PMID: 15091141. [PubMed: 15091141]
43. Kelly JL, Lyons A, Soberg CC, Mannick JA, Lederer JA. Anti-interleukin-10 antibody restores burn-induced defects in T-cell function. Surgery. 1997;122:146–152. PubMed PMID: 9288117. [PubMed: 9288117]
44. O'Suilleabhain C, O'Sullivan ST, Kelly JL, Lederer J, Mannick JA, Rodrick ML. Interleukin-12 treatment restores normal resistance to bacterial challenge after burn injury. Surgery. 1996;120:290–296. PubMed PMID:8751595. [PubMed: 8751595]
45. Panfoli I, Santucci L, Bruschi M, et al. Microvesicles as promising biological tools for diagnosis and therapy. Expert Rev Proteomics. 2018;15:801–808. Epub 2018/09/27. PubMed PMID: 30253662. [PubMed: 30253662]

46. Raeven P,Zipperle J, Drechsler S. Extracellular vesicles as markers and mediators in sepsis. Theranostics. 2018;8:3348–3365. PubMed PMID: 29930734; PMCID: 6010985. [PubMed: 29930734]
47. Yamamoto S, Azuma E, Muramatsu M, Hamashima T, Ishii Y, Sasahara M. Significance of extracellular vesicles: pathobiological roles in disease. Cell Struct Funct. 2016;41:137–143. PubMed PMID: 27679938. [PubMed: 27679938]
48. Buzas EI,Gyorgy B, Nagy G, Falus A, Gay S. Emerging role of extracellular vesicles in inflammatory diseases. Nat Rev Rheumatol. 2014;10:356–364. PubMed PMID: 24535546. [PubMed: 24535546]
49. Tetta C, Ghigo E, Silengo L, Deregibus MC, Camussi G. Extracellular vesicles as an emerging mechanism of cell-to-cell communication. Endocrine. 2013;44:11–19. PubMed PMID: 23203002; PMCID: 3726927. [PubMed: 23203002]
50. Burnouf T, Chou ML, Goubran H, Cognasse F, Garraud O, Seghatchian J. An overview of the role of microparticles/microvesicles in blood components: are they clinically beneficial or harmful?. Transfus Apher Sci. 2015;53:137–145. PubMed PMID: 26596959. [PubMed: 26596959]
51. van Niel G, D'Angelo G, Raposo G. Shedding light on the cell biology of extracellular vesicles. Nat Rev Mol Cell Biol. 2018;19:213–228. PubMed PMID: 29339798. [PubMed: 29339798]
52. Hreggvidsdottir HS, Ostberg T, Wahamaa H, et al. The alarmin HMGB1 acts in synergy with endogenous and exogenous danger signals to promote inflammation. J Leukoc Biol. 2009;86:655–662. PubMed PMID: 19564572. [PubMed: 19564572]
53. Sha Y, Zmijewski J, Xu Z, Abraham E. HMGB1 develops enhanced proinflammatory activity by binding to cytokines. J Immunol. 2008;180:2531–2537. PubMed PMID: 18250463. [PubMed: 18250463]
54. Ardoin SP, Pisetsky DS. The role of cell death in the pathogenesis of autoimmune disease: hMGB1 and microparticles as intercellular mediators of inflammation. Mod Rheumatol. 2008;18:319–326. Epub 2008/04/18. PubMed PMID: 18418695; PMCID: PMC2516192. [PubMed: 18418695]
55. Barnay-Verdier S, Gaillard C, Messmer M, Borde C, Gibot S, Marechal V. PCA-ELISA: a sensitive method to quantify free and masked forms of HMGB1. Cytokine. 2011;55:4–7. Epub 2011/04/09. PubMed PMID: 21474328. [PubMed: 21474328]
56. Kulkarni MM. Digital multiplexed gene expression analysis using the NanoString nCounter system. Curr Protoc Mol Biol. 2011. Chapter 25:Unit25B 10. PubMed PMID: 21472696.
57. Abdel-Hafez NM, Saleh Hassan Y, El-Metwally TH. A study on biomarkers, cytokines, and growth factors in children with burn injuries. Ann Burns Fire Disasters. 2007;20:89–100. Epub 2007/06/30. PubMed PMID: 21991076; PMCID: PMC3188064. [PubMed: 21991076]
58. Ozbalkan Z, Aslar AK, Yildiz Y, Aksaray S. Investigation of the course of proinflammatory and anti-inflammatory cytokines after burn sepsis. Int J Clin Pract. 2004;58:125–129. Epub 2004/04/02. PubMed PMID: 15055859. [PubMed: 15055859]
59. Finnerty CC, Przkora R, Herndon DN, Jeschke MG. Cytokine expression profile over time in burned mice. Cytokine. 2009;45:20–25. Epub 2008/11/21. PubMed PMID: 19019696; PMCID: PMC2668870. [PubMed: 19019696]
60. Finnerty CC, Herndon DN, Przkora R, et al. Cytokine expression profile over time in severely burned pediatric patients. Shock. 2006;26:13–19. Epub 2006/06/20. PubMed PMID: 16783192. [PubMed: 16783192]
61. Stanojcic M, Abdullahi A, Rehou S, Parousis A, Jeschke MG. Pathophysiological response to burn injury in adults. Ann Surg. 2018;267:576–584. Epub 2018/02/07. PubMed PMID: 29408836. [PubMed: 29408836]
62. Segura-Lepe MP, Keun HC, Ebbels TMD. Predictive modelling using pathway scores: robustness and significance of pathway collections. BMC Bioinformatics. 2019;20:543. Epub 2019/11/07. PubMed PMID: 31684857; PMCID: PMC6827178. [PubMed: 31684857]
63. Mobarrez F, Vikerfors A, Gustafsson JT, et al. Microparticles in the blood of patients with systemic lupus erythematosus (SLE): phenotypic characterization and clinical associations. Sci Rep. 2016;6:36025. PubMed PMID: 27777414; PMCID: PMC5078765. [PubMed: 27777414]

64. Pisetsky DS. The expression of HMGB1 on microparticles released during cell activation and cell death in vitro and in vivo. Mol Med. 2014;20:158–163. PubMed PMID: 24618884; PMCID: 4002850. [PubMed: 24618884]

65. Tricarico C, Clancy J, D'Souza-Schorey C. Biology and biogenesis of shed microvesicles. Small GTPases. 2017;8:220–232. Epub 2016/08/06. PubMed PMID: 27494381; PMCID: PMC5680703. [PubMed: 27494381]

66. Rice TC, Pugh AM, Xia BT, et al. Bronchoalveolar lavage microvesicles protect burn-injured mice from pulmonary infection. J Am Coll Surg. 2017;225:538–547. PubMed PMID: 28690205; PMCID: PMC5614837. [PubMed: 28690205]

67. O'Dea KP, Porter JR, Tirlapur N, et al. Circulating microvesicles are elevated acutely following major burns injury and associated with clinical severity. PLoS One. 2016;11:e0167801. PubMed PMID: 27936199; PMCID: 5148002. [PubMed: 27936199]

68. Skotland T, Sagini K, Sandvig K, Llorente A. An emerging focus on lipids in extracellular vesicles. Adv Drug Deliv Rev. 2020;159:308–321. Epub 2020/03/11. PubMed PMID: 32151658. [PubMed: 32151658]

69. Eckmann L, Kagnoff MF, Fierer J. Epithelial cells secrete the chemokine interleukin-8 in response to bacterial entry. Infect Immun. 1993;61:4569–4574. Epub 1993/11/01. PubMed PMID: 8406853; PMCID: PMC281206. [PubMed: 8406853]

70. Lippai D, Bala S, Petrasek J, et al. Alcohol-induced IL-1beta in the brain is mediated by NLRP3/ASC inflammasome activation that amplifies neuroinflammation. J Leukoc Biol. 2013;94:171–182. PubMed PMID: 23625200; PMCID: 3685015. [PubMed: 23625200]

71. Schwacha MG. Macrophages and post-burn immune dysfunction. Burns. 2003;29:1–14. Epub 2003/01/25. PubMed PMID: 12543039. [PubMed: 12543039]

72. Schwacha MG, Chaudry IH. The cellular basis of post-burn immunosuppression: macrophages and mediators. Int J Mol Med. 2002;10:239–243. Epub 2002/08/08. PubMed PMID: 12165794. [PubMed: 12165794]

73. Seok J, Warren HS, Cuenca AG, et al. Genomic responses in mouse models poorly mimic human inflammatory diseases. Proc Natl Acad Sci U S A. 2013;110:3507–3512. Inflammation, Host Response to Injury LSCRP. PubMed PMID: 23401516; PMCID: PMC3587220. [PubMed: 23401516]

74. Xiao W, Mindrinos MN, Seok J, et al. , Inflammation, Host Response to Injury Large-Scale Collaborative Research P. A genomic storm in critically injured humans. J Exp Med. 2011;208:2581–2590. PubMed PMID: 22110166; PMCID: 3244029. [PubMed: 22110166]

75. Schmidt K, Bruchelt G, Kistler D, Koslowski L. Phagocytic activity of granulocytes and alveolar macrophages after burn injury measured by chemiluminescence. Burns Incl Therm Inj. 1983;10:79–85. Epub 1983/11/01. PubMed PMID: 6652542. [PubMed: 6652542]

76. Hotchkiss RS, Coopersmith CM, McDunn JE, Ferguson TA. The sepsis seesaw: tilting toward immunosuppression. Nat Med. 2009;15:496–497. Epub 2009/05/09. PubMed PMID: 19424209; PMCID: PMC3786779. [PubMed: 19424209]

77. Martins PS, Brunialti MK, Martos LS, et al. Expression of cell surface receptors and oxidative metabolism modulation in the clinical continuum of sepsis. Crit Care. 2008;12:R25. Epub 2008/02/28. PubMed PMID: 18302745; PMCID: PMC2374621. [PubMed: 18302745]

78. Biswas SK, Chittezhath M, Shalova IN, Lim JY. Macrophage polarization and plasticity in health and disease. Immunol Res. 2012;53:11–24. Epub 2012/03/16. PubMed PMID: 22418728. [PubMed: 22418728]

79. Shapouri-Moghaddam A, Mohammadian S, Vazini H, et al. Macrophage plasticity, polarization, and function in health and disease. J Cell Physiol. 2018;233:6425–6440. Epub 2018/01/11. PubMed PMID: 29319160.

80. Chen MM, Bird MD, Zahs A, et al. Pulmonary inflammation after ethanol exposure and burn injury is attenuated in the absence of IL-6. Alcohol. 2013;47:223–229. Epub 2013/03/07. PubMed PMID: ; PMCID: PMC3617054. [PubMed: 23462222]

81. Accardo Palumbo A, Forte GI, Pileri D, et al. Analysis of IL-6, IL-10 and IL-17 genetic polymorphisms as risk factors for sepsis development in burned patients. Burns. 2012;38:208–213. [PubMed: 22079540]

82. Pileri D, Accardo Palombo A, D'Amelio L, et al. Concentrations of cytokines IL-6 and IL-10 in plasma of burn patients: their relationship to sepsis and outcome. Ann Burns Fire Disasters. 2008;21:182–185. Epub 2008/12/31. PubMed PMID: 21991134; PMCID: PMC3188197. [PubMed: 21991134]

83. Thery C, Witwer KW, Aikawa E, et al. Minimal information for studies of extracellular vesicles 2018 (MISEV2018): a position statement of the International Society for Extracellular Vesicles and update of the MISEV2014 guidelines. J Extracell Vesicles. 2018;7:1535750. Epub 2019/01/15. PubMed PMID: 30637094; PMCID: PMC6322352. [PubMed: 30637094]

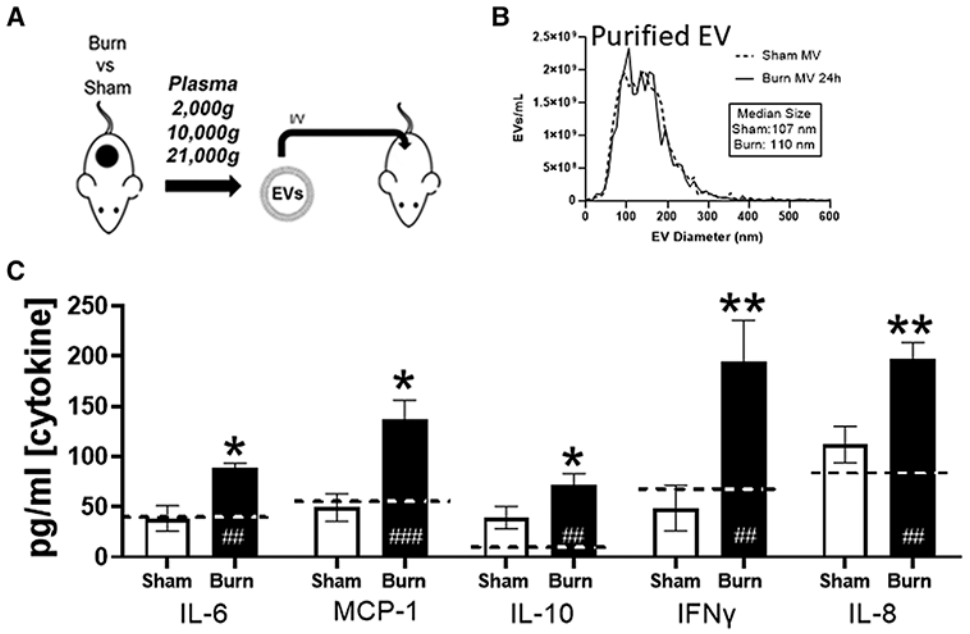

FIGURE 1. Extracellular vesicles (EVs) isolated from burnmice induce cytokine dysfunction upon adoptive transfer to uninjured mice in vivo.

(A) Experimental design. Mice underwent 20% total body surface area (TBSA) burn injury or sham injury and EVs were isolated from plasma (n = 12 mice per group) 48 h after injury. EVs were pooled from sham-injured (white bars) and burn-injured (black bars) mice (n = 6 per pool) were adoptively transferred into uninjured healthy mice (n = 3/group per experimental replicate) at a concentration of ~12.5% of baseline total circulating plasma EVs (10^{10}/mouse) i.v. by tail vein injection. Recipientmice were sacrificed 24 h after EV transfer. (B) Nanoparticle tracking analysis (NTA) analysis was to use to measure frequency and size distribution (i.e., diameter) of EVs isolated from burned and sham mice prior to transfer. No differences in size distributions of isolated EVs were found after burn or sham treatment. (B–G) Plasma concentrations of free cytokines after cell stimulation by burn EV (solid bars), sham EV (open bars), or untreated mice (dashed line) were measured by Bio-Plexmultiplex analysis. This experiment was performed in triplicate and data pooled, where *P < 0.05 and **P < 0.005 for burn EV-treated mice vs. sham EV-treated mice; ##P < 0.005 and ###P < 0.001 EV treated mice vs. normal, untreated mouse plasma levels of cytokine; n = 6/group *P < 0.05, t-tests with FDR q = 0.03

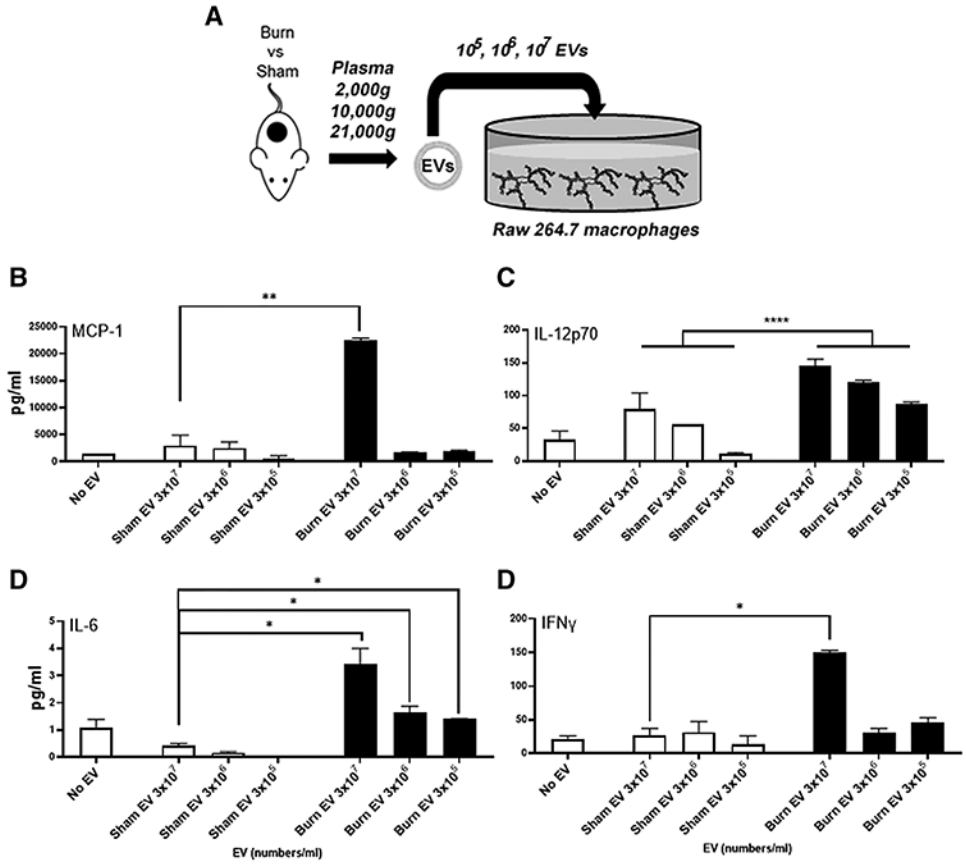

FIGURE 2. Extracellular vesicles (EVs) isolated early after burn-injuredmice (burn EVs) induce proinflammatory cytokines in RAW264.7 macrophages.

(A) Experimental design. Mice underwent a 20% total body surface area (TBSA) burn or sham injury with sacrifice at 24 h. EVs were isolated by differential centrifugation and different numbers (3×10^7, 3×10^6, or 3×10^5) added to adhered RAW264.7 macrophages (1×10^6 macrophages/well for 24 h). (B–E) A total of 24 h after EV transfer, cytokines and chemokines in RAWmacrophage media were measured by Bio-Plex multiplex analysis. Burn EVs induced significantlymore secretion of (B) MCP-1, 7.5-fold at 3×10^7, $^*P < 0.05$ vs. sham EV; (C) IL-12p70, 2-way ANOVA, main effect of treatment, $F_{1,7} = 70.45$, $^{****}P < 0.0001$ vs. sham; (D) IL-6, 8-fold at 3×10^7, $^*P < 0.05$ vs. sham; and (E) IFNγ, 5.8-fold at 3×10^7, $^*P < 0.05$ vs. sham. Data shown ± SEM; $^*P < 0.05$, $^{**}P < 0.01$ by Mann-Whitney unpaired nonparametric *t*-test unless otherwise noted. Key: sham injured (white bars) and burn injured (black bars). Each bar represents EVs from 12 source mice, with $n = 6$ different pooled EV preparations from 2 individual mice

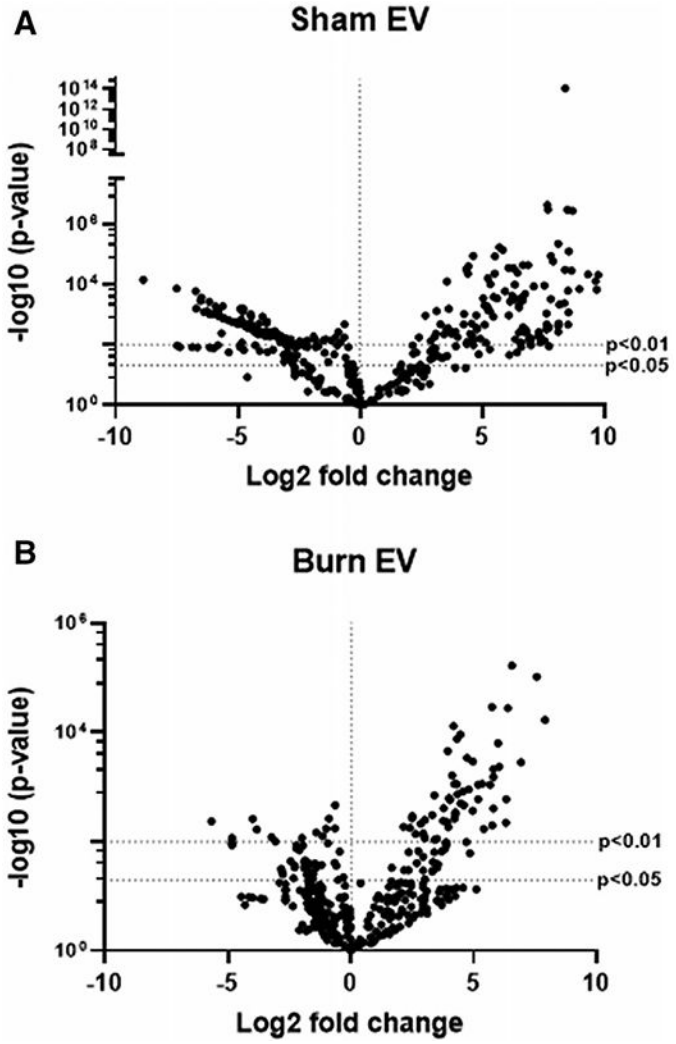

FIGURE 3. Extracellular vesicles (EVs) isolated from burn- or sham-injured mice differentially induce immune gene expression in macrophages.

mRNA was isolated from RAW264.7 cells exposed for 24 h to 3×10^5 EVs from burn- or sham-injured mice and gene expression evaluated using Nanostring barcoding spanning 561 mRNAs (nCounter Mouse Immunology CodeSet v3.0). Data are presented as the log2-transformed differential fold change in immune gene expression, with associated *P*-value significance (using Welch's *t*-test), after data normalization to housekeeping and internal control genes by nSolver v4.0. Differential fold change is macrophages exposed to (A) EVs isolated from sham-injured mice or (B) EVs isolated from burn-injured mice relative to cells not exposed to EV (each group represents cell cultures stimulated with EVs from 12 source mice, with $n = 6$ different pooled EV preparations from 2 individual mice). Significantly ($P < 0.01$) altered genes are presented in Supporting Information Table S1

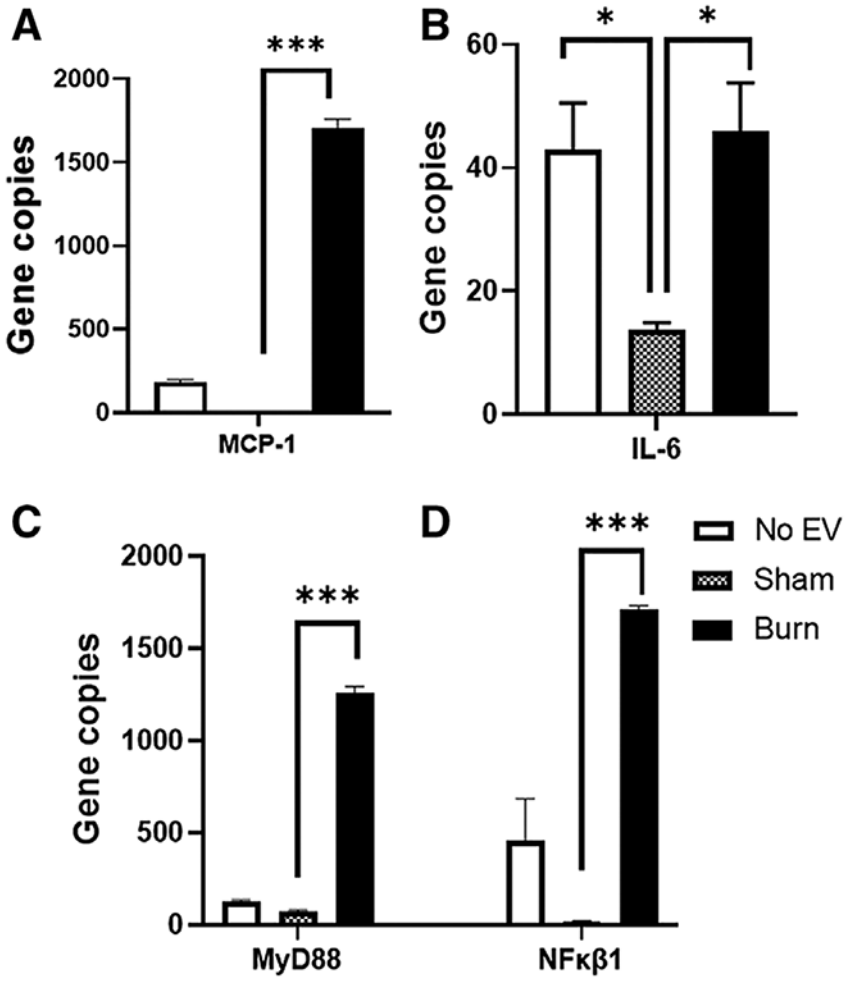

FIGURE 4. Extracellular vesicles (EVs) isolated from burn- or sham-injured mice induce significantly different levels of key innate immune genes inmacrophages.

mRNA was isolated from RAW264.7 cells exposed for 24 h to 3×10^5 EVs from burn-injured (black bars) or sham-injured (gray bars) mice or left unexposed (white bars) and gene expression was evaluated using Nanostring barcoding spanning 561 mRNAs (nCounter Mouse Immunology CodeSet v3.0). Evaluation of the normalized copy number found that burn EVs, promote up-regulation of (A) MCP-1, 17-fold; (B) IL-6, 3.3-fold; (C)MyD88, 24-fold; and (D) NFkB1, 150-fold (each group represents cell cultures stimulated with EVs from 12 source mice, with $n = 6$ different pooled EV preparations from 2 individual mice). Data are presented as the gene copy number of MCP-1, IL-6,MyD88, and NFkB1 after data normalization to housekeeping and internal control genes by nSolver v4.0. Data shown ± SEM; $*P < 0.05$, $**P < 0.01$, $***P < 0.005$ by Mann-Whitney unpaired nonparametric *t*-test

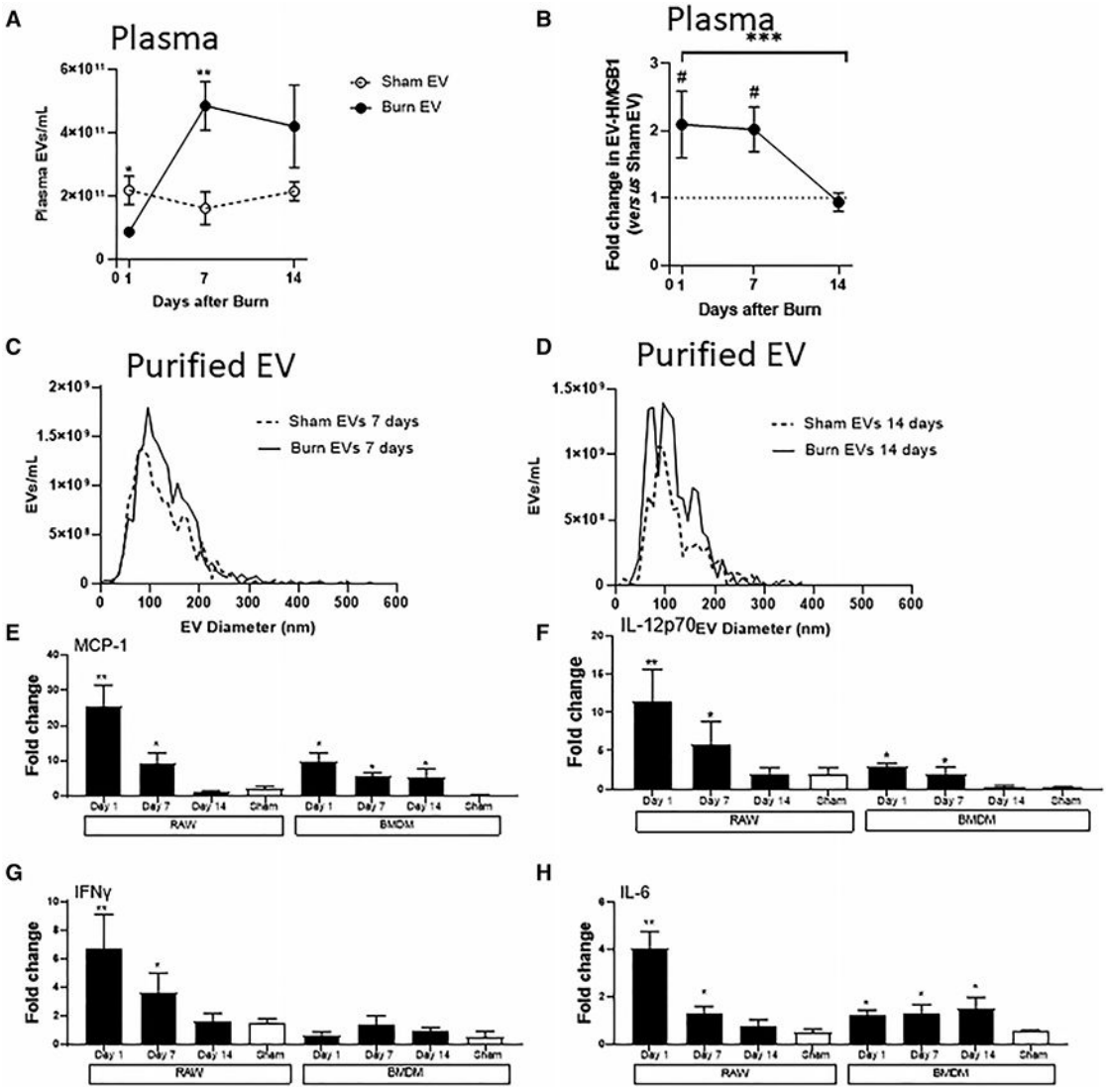

FIGURE 5. Extracellular vesicles (EVs) isolated after burn injury induce altered cytokine secretion patterns bymacrophages in vitro.

Mice underwent 20% total body surface area (TBSA) burn injury or sham injury, and blood harvested at days 1, 7, and 14 after injury. Burn mice had significantly different concentrations or EVs as determined by nanoparticle tracking analysis (NTA) (A), and high-mobility group protein 1 (HMGB1) cargo (B), as determined by ELISA vs. shammice (C) (data represent $n = 6$ mice per time point, ±SEM; A) $^{*}P < 0.05$, $^{**}P < 0.01$ by Mann-Whitney unpaired nonparametric t-test and B) $^{***}P < 0.0005$ by Mann-Whitney unpaired nonparametric t-test day 1 vs. day 14 burn EV, and $^{\#\#\#}P < 0.0005$ by Mann-Whitney unpaired nonparametric t-test day 7 vs. sham EV). NTA analysis was to use to measure size distribution (i.e., diameter) after purification from plasma. EVs isolated from plasma (C) 7 d or (D) 14 d after burn or sham injury showed similar size distributions compared to sham EV controls. (E–G) Equivalent numbers of EVs (3×10^7) isolated from sham-injured (white bars) and burn-injured (black bars) mice at each time point after burn injury were added to 1×10^6 adhered RAW264.7 or bone marrow-derived macrophages (BMDMs) for 24 h (each

bar represents 12 source mice, with $n = 6$ different pooled EV preparations from 2 individual mice). Supernatant cytokinesMCP-1, IL-6, IFNγ, and IL-12p70 were measured by Bio-Plex multiplex analysis. Data shown ± SEM; *$P < 0.05$, **$P < 0.01$ by Mann-Whitney unpaired nonparametric *t*-test

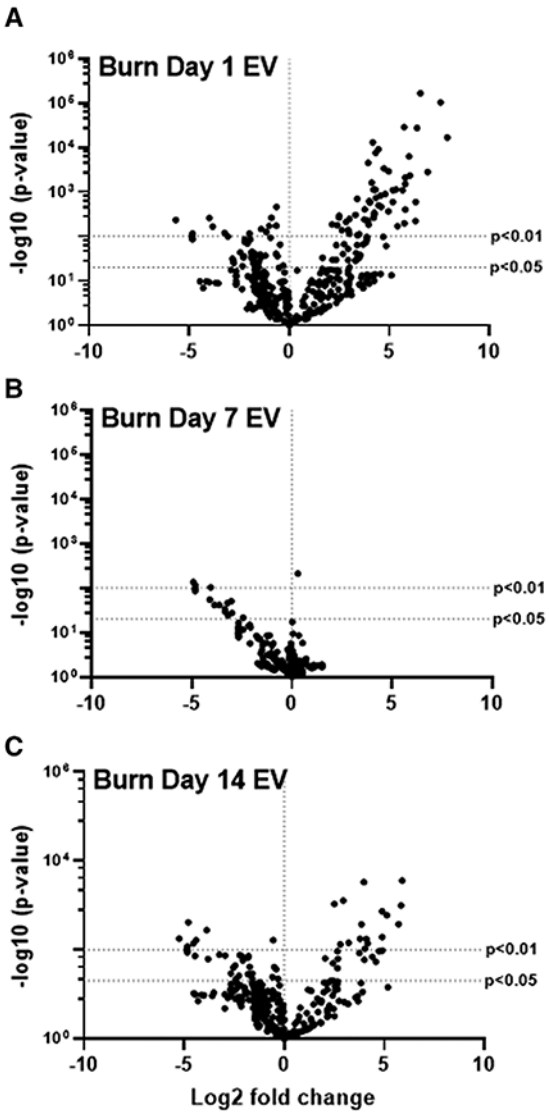

FIGURE 6. Extracellular vesicles (EVs) isolated from key time points after burn injury induce different immune gene signatures in macrophages vs. mRNA was isolated from RAW264.7 cells exposed for 24 h to 3 × 10^5 EVs isolated from plasma 1, 7, and 14 d after burn injury (*n* = 6 mice per time point).

Gene expression was evaluated using Nanostring barcoding spanning 561 mRNAs (nCounter Mouse Immunology CodeSet v3.0). Data are presented as the log2-transformed differential fold change in immune gene expression, with associated *P*-value significance (using Welch's *t*-test), after data normalization to housekeeping and internal control genes by nSolver v4.0. Differential fold change is macrophages exposed to EVs isolated (A) 1 d, (B) 7 d, and (C) 14 d following burn injury relative to cells not exposed to EV. Each group represents cell cultures stimulated with EVs from 12 source mice, with $n = 6$ different pooled EV preparations from 2 individual mice. Significantly ($P < 0.01$) altered genes are presented in Supporting Information Table S2

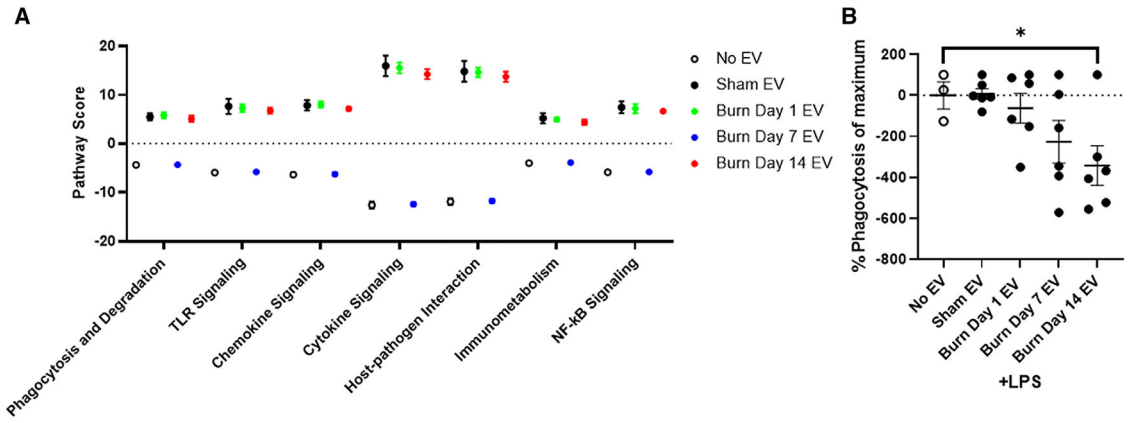

FIGURE 7. Extracellular vesicles (EVs) isolated from key time points after burn injury differentially induce macrophage innate immune phenotype and function.

(A) mRNA was isolated from RAW264.7 cells exposed for 24 h to 3×10^5 EVs isolated from the plasma 1, 7, and 14 d after burn injury ($n = 6$ mice per time point). Gene expression was evaluated using Nanostring barcoding spanning 561 mRNAs (nCounter Mouse Immunology CodeSet v3.0). Pathway scores (PS) from principal components analysis (PCA) of the gene expression data were generated utilizing nSolver v4.0 and R. These scores are based on the individual gene expression levels for all the measured genes within specific pathways.Open circle = no EVs; black = sham-EVs; green = burn-EVs day 1; blue = burn-EVs day 7; and red = burn-EVs day 14. Each group represents cell cultures stimulated with EVs from 12 source mice, with $n = 6$ different pooled EV preparations from 2 individualmice. (B) RAW264.7macrophages were incubated with 10 μg/ml LPS and fluorescein-labeled killed *E. coli* (K-12 strain) cells, in the presence or absence of 3×10^7 EVs isolated frommice day 1, 7, or 14 d after burn injury or EVs isolated from sham-injured mice (EVs from $n = 6$ mice per group). After 2 h of phagocytosis, and quenching of extracellular *E. coli* fluorescence, internalized *E.coli* was quantified. Data shown ± SEM; $^*P < 0.05$ by Mann-Whitney unpaired nonparametric *t*-test

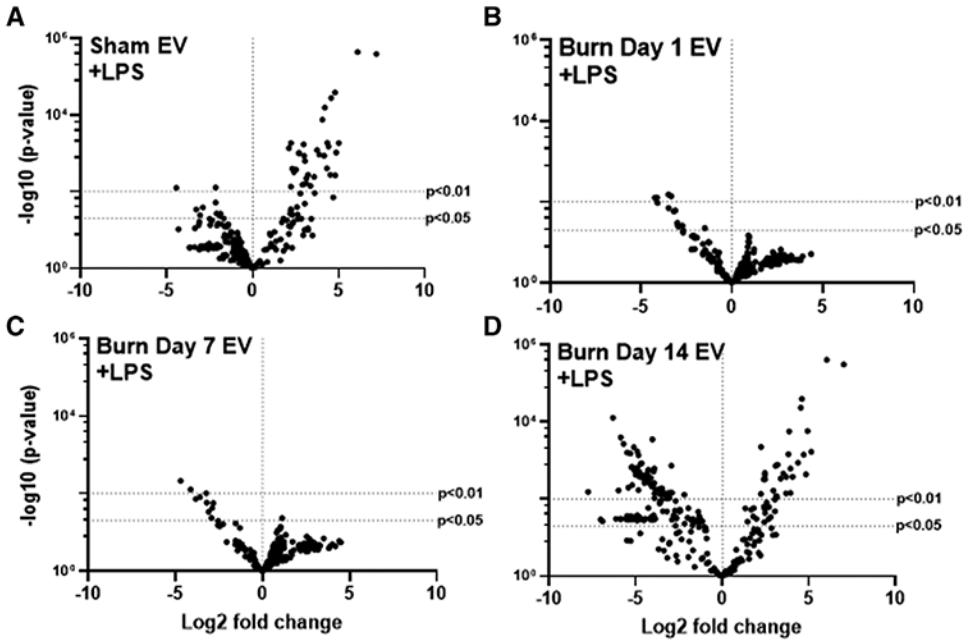

FIGURE 8. Extracellular vesicles (EVs) isolated from key time points after burn injury differentially shape LPS-inducedmacrophage innate immune gene signatures.

mRNA was isolated from RAW264.7 cells stimulated with 1 μg/ml LPS for 24 h in the presence or absence of 3×10^5 EVs isolated from the plasma 1, 7, and 14 d after burn injury ($n = 6$ mice per time point). Gene expression was evaluated using Nanostring barcoding spanning 561 mRNAs (nCounter Mouse Immunology CodeSet v3.0). Data are presented as the log2-transformed differential fold change in immune gene expression, with associated *P*-value significance (using Welch's *t*-test), after data normalization to housekeeping and internal control genes by nSolver v3.0. Each group represents cell cultures stimulated with EVs from 12 source mice, with $n = 6$ different pooled EV preparations from 2 individual mice. Differential fold change is LPS-stimulated macrophages exposed to EVs isolated (A) 1 d, (B) 7 d, and (C) 14 d following burn injury relative to LPS-stimulated cells not exposed to EV. Significantly ($P < 0.01$) altered genes are presented in Supporting Information Table S3

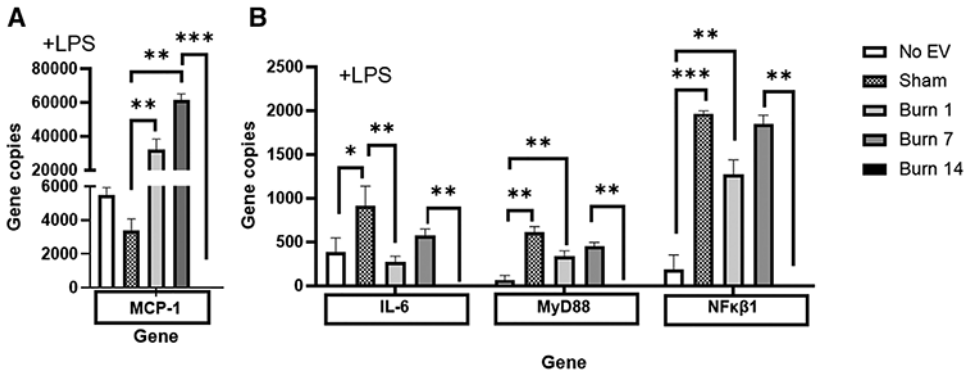

FIGURE 9. Extracellular vesicles (EVs) isolated from key time points after burn injury induce significantly different levels of LPS-responsive innate immune genes inmacrophages in vitro.

mRNA was isolated from RAW264.7 cells stimulated with 1 μg/ml LPS for 24 h in the presence or absence of 3×10^5 EVs isolated from the plasma 1, 7, and 14 d after burn injury (each group represents cell cultures stimulated with EVs from 12 source mice, with $n = 6$ different pooled EV preparations from 2 individual mice). Gene expression was evaluated using Nanostring barcoding spanning 561 mRNAs (nCounter Mouse Immunology CodeSet v3.0). Data are presented as the gene copy numbers of MCP-1, IL-6, MyD88, and NFkB1 after data normalization to housekeeping and internal control genes by nSolver v4.0. Data shown ± SEM; $*P < 0.05$, $**P < 0.01$, $***P < 0.005$ by Mann-Whitney unpaired nonparametric *t*-test

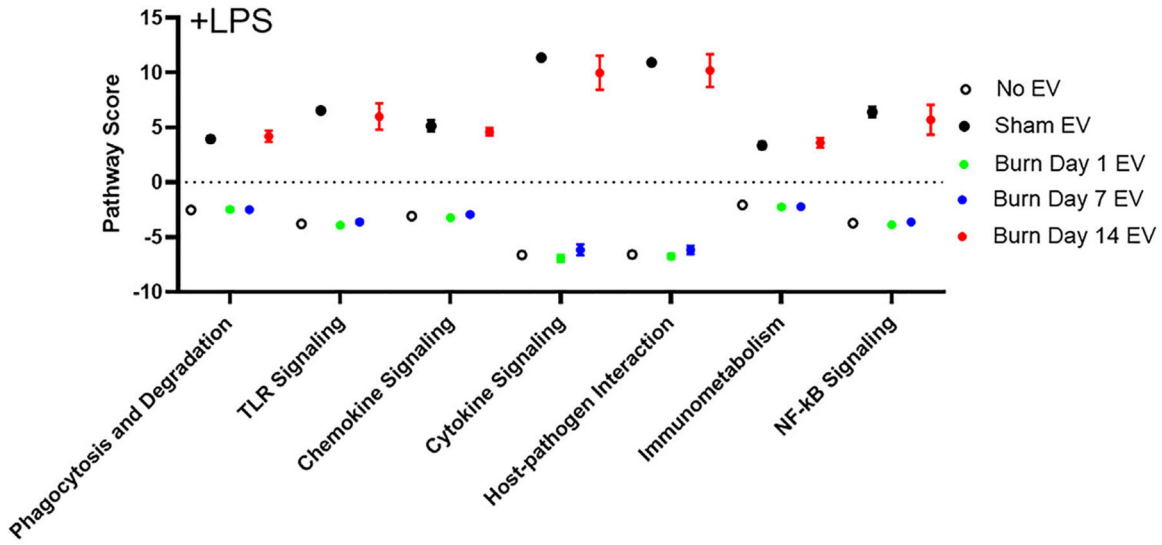

FIGURE 10. Extracellular vesicles (EVs) isolated from key time points after burn injury differentially shape LPS-induced immune function pathway scores (PS) in macrophages.

mRNA was isolated from RAW264.7 cells stimulated with 1 μg/ml LPS for 24 h in the presence or absence of 3×10^5 EVs isolated from the plasma 1, 7, and 14 d after burn injury ($n = 6$ mice per time point). Gene expression was evaluated using Nanostring barcoding spanning 561 mRNAs (nCounter Mouse Immunology CodeSet v3.0). PS from principal components analysis (PCA) of the gene expression data were generated utilizing nSolver v4.0 and R. Each group represents cell cultures stimulated with EVs from 12 source mice, with $n = 6$ different pooled EV preparations from 2 individual mice. These scores are based on the individual gene expression levels for all the measured genes within specific pathways. Open circle = no EV; black = sham-EV; green = burn-EVs day 1; blue = burn-EVs day 7; and red = burn-EVs day 14

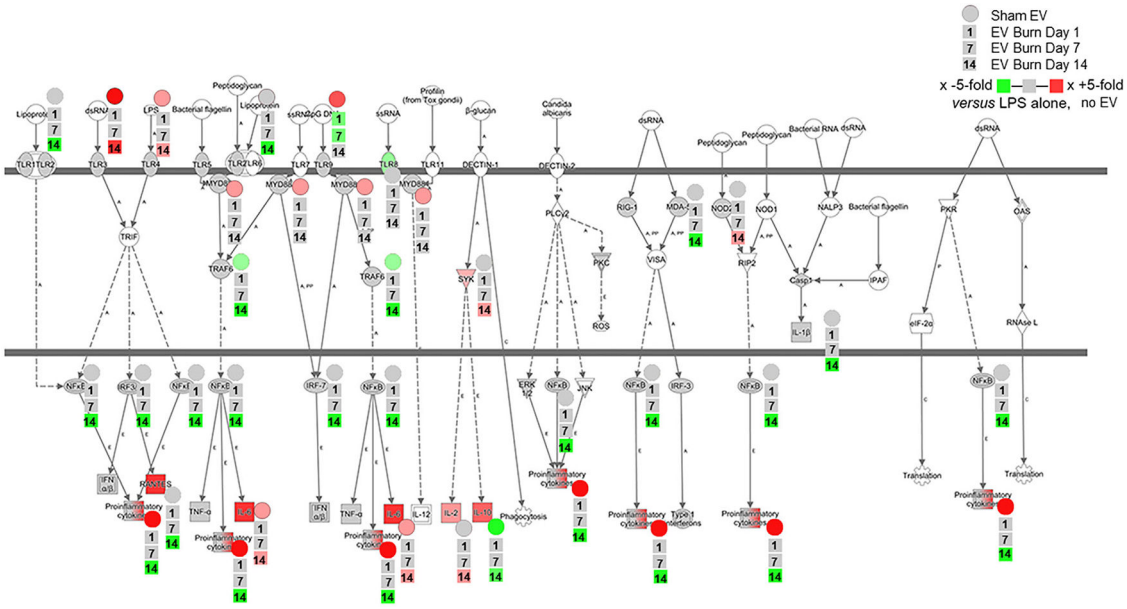

FIGURE 11. Extracellular vesicles (EVs) isolated from key time points after burn injury induce differential gene expressions, predicted to significantly impact immune functions in macrophages in vitro.

mRNA was isolated from RAW264.7 cells stimulated with 1 μg/ml LPS for 24 h in the presence or absence of 3×10^5 EVs isolated from the plasma 1, 7, and 14 d after burn injury ($n = 6$ mice per time point ingenuity pathways analysis was employed to detect and visualize the significant changes in expression of genes within the key macrophage innate immune pathway of pattern recognition receptor (PRR) signaling. Each group represents cell cultures stimulated with EVs from 12 source mice, with $n = 6$ different pooled EV preparations from 2 individual mice. The baseline data visualized is the fold change in specific genes after LPS stimulation in the absence of EV, relative to unstimulated cells in the absence of EV. Fold change in gene expression in the presence of EVs from sham injury (circle) or burn injury (squares) relative to LPS-stimulated cells in the absence of EV is indicated by increasing green representing increasing down-regulation, increasing red representing increased up-regulation, and gray representing no change in expression. For each gene that is significantly impacted by the addition of EVs, we have overlaid to the lower right of each gene symbol the immunomodulation of each EV type (from top to bottom, sham EVs (●), and then burn EVs from each time point after injury (■) days 1, 7, and 14 (stacked in the order shown in the legend)

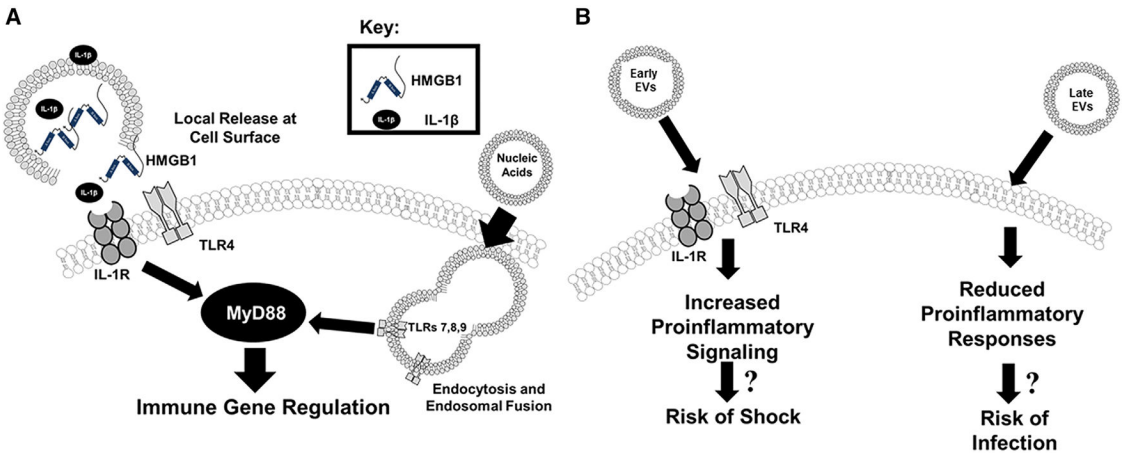

FIGURE 12. Summary figure.

Extracellular vesicles (EVs), (A) induce immune regulation via multiple mechanisms, and (B) when isolated from key time points after burn injury induce differential gene expression mirroring the clinical phenotype associated with burn injury